



THE UNIVERSITY *of* EDINBURGH

Edinburgh Research Explorer

Longitudinal zonation pattern in Arabidopsis root tip defined by a multiple structural change algorithm

Citation for published version:

Pacheco-Escobedo, M, Ivanov, V, Ransom-Rodríguez, I, Arriaga-Mejía, G, Ávila, H, Baklanov, I, Pimentel, A, Corkidi, G, Doerner, P, Dubrovsky, J, Álvarez-Buylla, E & Garay-Arroyo, A 2017, 'Longitudinal zonation pattern in Arabidopsis root tip defined by a multiple structural change algorithm' *Annals of Botany*. DOI: 10.1093/aob/mcw101

Digital Object Identifier (DOI):

[10.1093/aob/mcw101](https://doi.org/10.1093/aob/mcw101)

Link:

[Link to publication record in Edinburgh Research Explorer](#)

Document Version:

Peer reviewed version

Published In:

Annals of Botany

General rights

Copyright for the publications made accessible via the Edinburgh Research Explorer is retained by the author(s) and / or other copyright owners and it is a condition of accessing these publications that users recognise and abide by the legal requirements associated with these rights.

Take down policy

The University of Edinburgh has made every reasonable effort to ensure that Edinburgh Research Explorer content complies with UK legislation. If you believe that the public display of this file breaches copyright please contact openaccess@ed.ac.uk providing details, and we will remove access to the work immediately and investigate your claim.



Longitudinal zonation pattern in Arabidopsis root tip defined by a multiple structural change algorithm

Thank you for agreeing to review this paper for *Annals of Botany*.

We are aiming to be among the very top plant science journals, which currently means an Impact Factor greater than 4.5. We receive over 1000 submissions every year and we only have room to publish a limited number of these.

We therefore need to be very selective in deciding which papers we can publish, so in making your assessment please consider the following points.

- **We want to publish papers where our reviewers are enthusiastic about the science: is this a paper that you would keep for reference, or pass on to your colleagues?**

If the answer is “no” then please enter a low priority score when you submit your report.

- **We want to publish papers with novel and original content that move the subject forward, not ones that report incremental advances or findings that are already well known in other species.**

Please consider this when you enter a score for originality when you submit your report.

Notes on categories of papers

Research papers should demonstrate an important advance in the subject area, and the results should be clearly presented, novel and supported by appropriate experimental approaches. The Introduction should clearly set the context for the work and the Discussion should demonstrate the importance of the results within that context. Concise speculation, models and hypotheses are encouraged, but must be informed by the results and by the authors' expert knowledge of the subject.

Reviews should place the subject in context, include the most up-to-date references available and add significantly to previous reviews in the topic. An idea review will move forward research in the topic.

Research in Context should combine a review/overview of a subject area with original research that moves the topic forward; i.e. it is a hybrid of review/research papers.

Viewpoints should present clear, concise and logical arguments supporting the authors' opinions, and in doing so help stimulate discussions within the topic.

Special Issue/Highlight papers should be judged by the same standards as other papers in terms of the strength of the work they contain. They are allowed a more narrow focus within the topic of the issue in which they will appear. Special Issue papers should still make the topic of interest to a wide audience.

1 **Original Article**

2 **Longitudinal zonation pattern in *Arabidopsis* root tip defined by a multiple structural**
3 **change algorithm**

4 **Mario A. Pacheco-Escobedo^{1†}, Victor B. Ivanov^{2†}, Iván Ransom-Rodríguez¹, Germán**
5 **Arriaga-Mejía³, Hibels Ávila³, Ilya A. Baklanov², Arturo Pimentel⁴, Gabriel Corkidi⁴, Peter**
6 **Doerner⁵, Joseph G. Dubrovsky^{4*}, Elena R. Álvarez-Buylla^{1*}, Adriana Garay-Arroyo^{1*}**

7 ¹Laboratorio de Genética Molecular, Desarrollo y Evolución de Plantas, Instituto de Ecología,
8 Universidad Nacional Autónoma de México, 3er Circuito Ext. Junto a J. Botánico, Ciudad
9 Universitaria, UNAM, México DF, Mexico

10 ² Department of Root Physiology, Timiryazev Institute of Plant Physiology, Russian Academy of
11 Sciences, ul. Botanicheskaya 35, Moscow, 127276 Russia

12 ³ Escuela Superior de Física y Matemáticas, Instituto Politécnico Nacional, U.P. Adolfo López
13 Mateos, México DF, México.

14 ⁴ Instituto de Biotecnología, Universidad Nacional Autónoma de México, Apartado Postal 510-3,
15 62250 Cuernavaca, Morelos, México

16 ⁵ Institute of Molecular Plant Science, School of Biological Sciences, University of Edinburgh,
17 Edinburgh, UK.

18

19 **Running title:** Root Apex Zonation in arabidopsis

20 For Correspondence:

21 E-mail: jdubrov@ibt.unam.mx (JGD)

22 E-mail: eabuylla@gmail.com (ER AB)

23 E-mail: garay.adriana@gmail.com (AGA)

24 [†] These authors contributed equally to this work.

1
2
3
4
5
6
7
8
9
10
11
12
13
14
15
16
17
18
19
20
21
22

ABSTRACT

- **Background and Aims** The *Arabidopsis thaliana* (arabidopsis) root is a key experimental system in developmental biology. Despite its importance, we are still lacking an objective and broadly applicable approach for identification of number and position of developmental domains or zones along the longitudinal axis of the root apex or boundaries between them, which is essential for understanding the mechanisms underlying cell proliferation, elongation, and differentiation dynamics during root development.
- **Methods** We used a statistics approach, multiple structural change algorithm (MSC), for estimating the number and position of developmental transitions in the growing portion of the root apex. Once the positions of the transitions between domains and zones are determined, linear models are used to estimate the critical size of dividing cells (L_{critD}) and other parameters.
- **Key Results** MSC approach enabled identification of three discrete regions in the growing part of the root that correspond to the proliferation domain (PD), the transition domain (TD), and the elongation zone (EZ). Simultaneous application of MSC approach and G2-to-M transition (*CycB1*; *I_{DB}*:*GFP*) and endoreduplication (*pCCS52A1*:*GUS*) molecular markers confirmed the presence and position of the TD. We also found that MADS-box gene *XAANTALI* (*XAL1*) is required for the wild type (wt) PD increase in length during the first two weeks of growth. Contrary to wt, in the *xal1* loss-of-function mutant this increase and acceleration of root growth were not detected. We also found

1 alterations in *L_{critD}* in *xall* compared to wt which was associated with longer cell cycle
2 duration in the mutant.

3 • **Conclusions** The MSC approach is a useful, objective, and versatile tool for identification
4 of the PD, TD, and EZ and boundaries between them in the root apices and can be used
5 for phenotyping of different genetic backgrounds, experimental treatments or
6 developmental changes within a genotype. The tool is publicly available at
7 www.ibiologia.com.mx/MSA_analysis.

8 **Key words:** *Arabidopsis thaliana*, cell differentiation, cell proliferation, proliferation domain,
9 transition domain, elongation zone, root apical meristem, longitudinal zonation pattern, critical
10 size of dividing cells, *XAANTALI*, multiple structural change model, breakpoints.

11
12
13
14
15
16
17
18
19
20
21
22
23
24

INTRODUCTION

1
2 Plant growth and development are regulated by the combined activity of two processes that are
3 closely linked: cell division and cell elongation. Fully elongated cells undergo terminal
4 differentiation. Reliable and quantitative characterization of both processes in organs is thus
5 essential for understanding their role during development. The *Arabidopsis thaliana* (arabidopsis)
6 root is an important model system for molecular genetics and cellular studies of plant
7 development, including understanding cell cycle regulation and the balance of proliferation and
8 differentiation in complex organs. The root is an excellent model system, among other
9 characteristics, for its relatively simple longitudinal organization and the possibility of observing
10 different developmental stages in the same root along its longitudinal axis. Another advantage of
11 the root is that it has few cell types organized concentrically around the vascular tissues,
12 composed of xylem, phloem, vascular parenchyma and pericycle. Outside of the vascular tissues
13 there are concentric rings of cells of endodermis, cortex and epidermis covered at the very tip by
14 the lateral root cap and columella cells. The growing part of the root consists of two zones: the
15 root apical meristem (RAM) and the elongation zone (EZ) (Fig. 1A).

16 The RAM includes the proliferation domain (PD) where cells have a high probability of
17 dividing and the transition domain (TD) (Baluška et al., 1996). The most distal portion of the PD
18 contains the quiescent centre (QC), a stem cell niche, surrounded by the initial (stem) cells
19 (Clowes 1956; Dolan et al. 1993; Sabatini et al. 2003). In the TD domain cells can still divide but
20 at a low probability and continue elongating at the same low rate as in the PD. Hence, cells in this
21 domain are slightly longer than cells in the PD (Fig. 1B) (Ivanov and Dubrovsky 2013). The EZ
22 is the zone where cells of different tissues simultaneously start rapid elongation at rates much
23 higher than those in the RAM. The EZ is followed by the differentiation zone (DZ), where
24 elongated cells reach their final length and differentiation state. The rootward border of the DZ

1 corresponds to the position at which cell elongation ceases (van der Weele et al. 2003; Ivanov
2 and Dubrovsky 2013). Therefore, identification of the boundary between the EZ and DZ is
3 straightforward and is based on either cell length profile data or appearance of first root hair
4 bulges, which is a hallmark of termination of elongation (Dolan et al. 1993; Ma et al. 2003;
5 Dolan and Davies 2004). Despite the importance of being able to fully characterize the apical-
6 basal patterning of the root tip, no consensus on the domains and zones in the arabidopsis root
7 apex has been attained (Ivanov and Dubrovsky 2013). Here, we applied a statistical algorithm for
8 determining the number of zones and domains in the growing part of the root and the limits
9 between neighbouring zones and domains. Our results support the existence of three discrete
10 regions in the growing part of the arabidopsis root: the PD, the TD and the EZ.

11 A rigorous qualitative and quantitative description of these zones and domains, and
12 identification of their boundaries are essential for understanding the effects of different genetic,
13 chemical and physical alterations of cell proliferation, growth, and differentiation during root
14 growth and development. Comparisons between different experimental conditions require
15 approaches that enable accurate evaluations of the size and number of cells within the RAM or its
16 PD. This is generally done in the cortex cell layer (Casamitjana-Martínez et al. 2003; Dello Ioio
17 et al. 2007; Tsukagoshi et al. 2010; Zhou et al. 2011; Garay-Arroyo et al. 2013). However, the
18 lack of objective criteria and subjectivity in identifying the boundaries between root growth zones
19 and domains indicate the need for development of new approaches.

20 Several previous papers have approached this problem. For example, Scheres and
21 collaborators (Casamitjana-Martínez et al. 2003), determine the boundary between the RAM and
22 the EZ (RAM/EZ boundary) as the point where cells begin to increase significantly their lengths.
23 The onset of rapid cell elongation and absence of cell division in the EZ are taken as the only
24 criteria to distinguish between these two regions. Although useful for rough qualitative

1 evaluations, without measuring cell lengths, the identification of the point where rapid elongation
2 starts may vary among researches. A relatively more objective way of determining this boundary
3 implies finding the position at which cell length in a file is more than twice than that of the
4 previous cell (González-García et al. 2011). The latter method may yield biased results: before
5 rapid elongation starts, a longer cell can be followed by a shorter cell in the TD, indicating that
6 this criterion is not always sufficient for an objective establishment of the RAM/EZ boundary.
7 Recently, a geometric approach for identification of the point at which cell elongation starts was
8 proposed that yields similar results to those obtained arbitrarily (French et al. 2012). This and
9 other studies (Dello Ioio et al. 2007; Moubayidin et al. 2010; Tsukagoshi et al. 2010) do not
10 specify how to identify the border between the PD and the TD of the RAM (the PD/TD
11 boundary). Changes in cell proliferation precede the transition to rapid cell elongation: the
12 mitotic index (percentage of dividing cells) decreases drastically (Ivanov and Dubrovsky 2013)
13 and endoreduplication starts (Hayashi et al. 2013). For that reason, the PD/TD boundary is
14 associated with changes in cell proliferation, whereas the RAM/EZ boundary defines the point
15 where drastic shift to rapid elongation occurs.

16 The position of the PD/TD boundary is particularly difficult to establish because it
17 fluctuates in time within a cell file and, additionally, is frequently different among different files
18 of cells of the same or different types (Baluška and Mancuso 2013; Ivanov and Dubrovsky 2013).
19 Because of this, the PD/TD boundary can only be approximated with certain error that should be
20 estimated (Ivanov and Dubrovsky 2013). The position of this boundary can be determined as the
21 point where average cell length along the RAM has slightly increased, or where the distances
22 between nuclei in neighbouring cells along a cell file become greater than the diameter of the
23 nuclei (Rost and Baum 1988; Dubrovsky et al. 1998a, 1998b; Garay-Arroyo et al. 2013). It is also
24 possible to locate the beginning of the TD as the position where the mitotic index sharply

1 decreases for the tissue under consideration (Ivanov and Dubrovsky 2013). Nonetheless, the latter
2 approach is difficult to implement and it is not valid for all species. All such criteria can lead to
3 variable and subjectively defined boundaries and/or require considerable experience from the
4 researcher in order to guarantee reproducible and reliable data. Because of the importance of each
5 of the root developmental domains and/or zones in the cell proliferation/differentiation balance
6 (Dello Ioio et al. 2007; Moubayidin et al. 2010; Tsukagoshi et al. 2010), establishing the PD/TD
7 and RAM/EZ boundaries is essential for a complete phenotypical description of the root. This
8 requires a quantitative approach, which enables the unambiguous identification of the different
9 development stages along the root longitudinal axis.

10 Here, to identify the location of the PD/TD and RAM/EZ boundaries we applied a
11 multiple structural change algorithm (MSC) to cell length profile data collected on fixed root
12 preparations. Because the position of the EZ/DZ boundary corresponds to the location where root
13 hair formation starts, this location can be used as a qualitative criterion for determination the
14 shootward border of the EZ. For this reason the EZ/DZ boundary can be easily established, and is
15 not considered in this study. We show here that using the polygonal models obtained from a
16 MSC algorithm it is possible to estimate: (a) the lengths of the PD, the TD and the EZ; (b) the
17 distances from the QC at which the different developmental transitions start; (c) the critical sizes
18 of dividing and transitioning to the EZ cells; (d) the derivative of cell length as a function of
19 position or gradient in cell length (Silk et al. 1986). We also show that the MSC yields similar
20 results to those obtained with molecular markers that have been used to determine the PD/TD
21 boundary, as well as those obtained by arbitrary estimations made by researchers experienced in
22 root developmental biology.

23 *XAANTALI* (*XALI*) or *AGLI2* is a member of the MADS-box family of genes that encode
24 transcription factors important for regulating plant and animal development. This gene

1 participates in the regulation of cell proliferation in the arabidopsis RAM (Tapia-López et al.
2 2008). Loss-of-function alleles have shorter roots and lower root growth rates than wt explained
3 by a shorter RAM, lower rates of cell production, and a longer cell cycle duration than wt roots
4 (Tapia-López et al. 2008). We used the proposed MSC approach to analyse arabidopsis wt and
5 loss-of-function allele *xal1-2* (hereafter *xal1*) roots. We found that *XALI* is necessary for the
6 increase of the length of the PD during the first days after seed germination and its loss of
7 function altered the critical size of dividing cells. This example illustrates that MSC approach is
8 useful for root phenotyping at the cellular level, for comparing of different experimental
9 conditions or genotypes and can be applied to better understand the changes in cell growth rates,
10 the distribution of cell divisions, changes in the critical size of dividing cells and longitudinal
11 zonation pattern.

12

13

MATERIALS AND METHODS

Plant materials and growth conditions

14 *Arabidopsis wild type, xal1-2, CycB1;I_{DB}:GFP* and *pCCS52A1:GUS* are in Col-0 ecotype. C24
15 and Col-0 were obtained from the [Arabidopsis Biological Resource Center](#) at the Ohio State
16 University. Seeds carrying *pCCS52A1:GUS* were kindly donated by E. Kondorosi, and
17 *CycB1;I_{DB}:GFP* was constructed by P. Doerner (Ubeda-Tomás et al. 2009). All lines were
18 homozygous; seeds were surface sterilized and 2 days after vernalisation sown on medium
19 containing 0.2X MS salts, 1% sucrose and 1% agar (except for *CycB1;I:GFP* seeds; see below).
20 Petri dishes were maintained in vertical position. Plants were grown under long-day (16 h light/8
21 h dark) conditions in growth chambers at 22-24 °C. Seeds of *CycB1;I_{DB}:GFP* line were plated on
22 agar media N103 and N3003 that contained 0.3% sucrose supplemented with 1 (N103) or 30
23 (N3003) mM of total nitrogen (final concentrations of other components of the media were:
24

1 CaCl₂ [3 mM], MgSO₄ [1.5 mM], KH₂PO₄ [1.5 mM], 1 x MS microelements, MES [5 mM],
2 sucrose, 3 g/l, pH 5.6). After 2 to 7 days of vernalisation, plates were transferred to growth
3 chambers and grew at constant light in vertically maintained Petri dishes. Root growth
4 increments were recorded daily by marking root tip position over the surface of the dish and
5 increments were measured using ImageJ (<http://rsb.info.nih.gov/ij>).

6

7 *Microscopy*

8 In seedlings of 7 or 9 days after sowing (DAS) roots were cleared using Herr's solution (Herr
9 1971), that contains: lactic acid (85%), chloral hydrate, phenol, clove oil, and xylene (2:2:2:2:1,
10 by weight). Excised roots were transferred to Herr's solution for at least 24 h at room temperature
11 and subsequently mounted in the same solution and visualized using Olympus BX60 microscope
12 equipped with Nomarski optics and photographed.

13 *pCCS52A1:GUS* seedlings were subjected to GUS reaction in the dark for 1 h at 37 °C
14 and GUS staining solutions were prepared as described by Malamy and Benfey (1997). To
15 restrict the diffusion of GUS blue precipitate, 2 mM of K₃Fe(CN)₆ and K₄Fe(CN)₆ were added in
16 the solution at the beginning. After GUS staining, seedlings were immersed in Herr's clearing
17 solution and stored in the dark at room temperature during 72 h and visualised as described
18 above.

19 For simultaneous observation of the nuclei and GFP fluorescence (*CycB1; I_{DB}:GFP*), 7
20 DAS seedlings were fixed in 4% formaldehyde in PBS solution supplemented with 0.05 µg/ml of
21 DAPI (final concentrations) overnight at 4 °C. Preliminary experiments showed that this
22 procedure did not quench fluorescence activity of GFP. Then, material was washed in PBS four
23 times, 10 min each, mounted and analysed. Roots were mounted in a drop of PBS, covered by a
24 coverslip and observed under inverted laser scanning confocal Leica TCS NT microscope with a

1 63X HCX PL APO water immersion Leica objective. After the optical median section of the
2 apical root portion was found, the intensity of the signal was set up with the use of look-up tables
3 which are the component of the Leica software. DAPI and GFP channels were setup separately
4 and colour intensity was always set to a standard for each individual root at low speed of
5 scanning. These same setting in colour intensity and offset were used for more proximal root
6 portions. Final scanning of each root portion was done sequentially, first for GFP and then for
7 DAPI and average of four scans was saved as TIF file. To improve contrast between DAPI and
8 GFP channel, images of GFP fluorescence were pseudo-coloured in magenta. Images of two
9 channels of each root portion were merged and then the whole root tip image was assembled in
10 Adobe Photoshop 5.5. from four to eight originally saved files.

11

12 *Quantitative analysis*

13 We have implemented a semi-automated procedure to systematically and accurately measure cell
14 lengths. The algorithm was constructed based on Java SRE and ImageJ 1.4 libraries. This
15 development works properly for multi-platform environments such as Windows, Linux or Mac
16 OS. This software (executable file: Cell_Length_V2.0.jar) and its user manual
17 (Cell_Length_V2.0.pdf) are available at

18 <http://www.ibt.unam.mx/labimage/proyectos/arabidopsis>.

19 For Nomarski micrographs, cell length profiles were obtained by measuring a straight line from
20 one end to the other with ImageJ or Cell_Length_V2.0.jar software along a cortex file from the
21 QC to the first cortex cell adjacent to an epidermal cell that had started to form a root hair bulge
22 (Fig. 1A). For confocal images the data on meristem length, number of cell in the meristem, the
23 fraction of GFP expressing cells, and root thickness were collected from assembled images. Root
24 thickness was measured at the level corresponding to the PD/TD boundary for cortex determined

1 by experienced biologists which implies a subjective method abbreviated here as the ExpBiol
2 method. The PD/TD boundary determined by an ExpBiol method was defined for epidermis and
3 cortex arbitrarily based on relative changes in cell lengths or internuclear distances along the root,
4 similar to other studies (Rost and Baum 1988; Dubrovsky 1997; Dubrovsky et al. 1998a, b;
5 Tapia-López et al. 2008; Garay-Arroyo et al. 2013).

6 All statistical analyses were performed using R (the R Foundation of Statistical
7 Computing, version 2.15.1). Multiple structural change (MSC) analyses, including estimation of
8 the optimal number of breakpoints by Bayesian Information Criterion (BIC) and estimation of
9 breakpoint positions with their 95% confidence intervals (CI) for all cell length profiles, were
10 performed using the *breakpoints* function of the R *strucchange* package (Zeileis et al. 2002,
11 2003). *breakpoints* function estimates multiple breakpoints simultaneously implementing the
12 algorithm which obtains global minimizers of the sum of squared residuals (Bai and Perron2003).
13 Examples of MSC analyses using the *breakpoints* function are provided [**Supplementary**
14 **Information**, Text S1]. The distribution function for the 95% CI for the breakpoints is given in
15 Bai (1997). For comparison of the results obtained with ExpBiol and MSC analyses, Intraclass
16 Correlation Coefficient (ICC) was estimated (the model: two-way; the type: absolute agreement;
17 the unit of analysis: average-measures) (McGraw and Wong 1996; Hallgren 2012). The ICC
18 value and its 95% CI were calculated using the R *irr* package (Matthias et al. 2012). We also
19 developed a publically available web site www.ibiologia.com.mx/MSC_analysis where the MSC
20 algorithm can be performed.

21
22
23
24

RESULTS

1
2 Previously, van der Weele and collaborators (2003) concluded that the root has a velocity profile
3 with linear phases —RAM, EZ and Differentiation zone— separated by abrupt transitions. Based
4 on this conclusion, we propose that cell length profiles, where the cell length (L) is a function of
5 the cell position with respect to the QC (i), can be fitted by a polygonal model, also known as
6 piecewise, segmented, broken-line regressions, multi-phase regressions or multiple structural
7 change (MSC) models (Bai and Perron 2003; Muggeo 2003). In these models the points where
8 the behaviour or response of the dependent variable, as a function of the independent one, change
9 abruptly are commonly called breakpoints, change-points, transition points or switch-points
10 (Muggeo 2003). In the cell length profiles, the breakpoints correspond to the boundary between
11 adjacent developmental zones (Fig. 1A, B).

12 There is no consensus about the existence of the TD in roots. Thus, the analysis of the
13 longitudinal zonation pattern of the arabidopsis root apex consists of two main problems:
14 establishing the number of domains and zones, and determination of the position of the
15 breakpoints between them. Here, we show that a MSC approach can be productively used for
16 solving these problems and objectively establishing the longitudinal patterning in the arabidopsis
17 growing root portion.

18

19 *The growing part of the root consists of three discrete regions*

20 The problem of single and multiple structural changes in linear models has been studied mainly
21 in statistics, econometrics and medicine (Auger and Lawrence 1989; Bai and Perron 1998, 2003;
22 Kim et al. 2000; Muggeo 2003). We know that the growing part of the arabidopsis root has at
23 least one transition or breakpoint that corresponds to the RAM/EZ boundary. Some authors
24 propose also the existence of a TD formed by a group of cells elongating at the same rate as the

1 PD cells but with a very low probability of division. In contrast, other authors consider that such
2 domain does not exist. If the TD actually exists, then a polygonal model with two breakpoints can
3 be obtained from cell length profiles of single cell files; and such breakpoints would correspond
4 to PD/TD and RAM/EZ boundaries.

5 There are several procedures to estimate the number of breakpoints in MSC models (Yao
6 1988; Liu et al. 1997; Bai and Perron 1998, 2003; Kim et al. 2000, 2009). Comparing different
7 methods for selecting the number of breakpoints, Bai and Perron (2003) concluded that the
8 Bayesian Information Criterion (BIC) (Yao 1988) works well when there is at least one
9 breakpoint, and Kim et al. (2009) also indicate that BIC performs well in picking up small
10 changes. This method adjusts the sum of squared residuals for models with different numbers of
11 breakpoints, and the model with the lowest BIC value is accepted as the most parsimonious. To
12 establish the number of regions in the growing part of the root, we analysed arabidopsis Col-0 wt
13 and *xall* roots at two different ages, 7 and 9 DAS, without specifying the number of expected
14 breakpoints. From cleared roots we obtained the cell length profile of a cortex cell file, from the
15 QC to the first cortex cell adjacent to an epidermal cell that formed a root hair bulge (Fig. 1A).
16 For each cell length profile we estimated MSC models with different number of breakpoints and
17 their positions.

18 We found that for 58% of Col-0 cell length profiles analysed (23 out of 40 cell files) the
19 most parsimonious model was of two breakpoints (Fig. 2A, B). In these cell length profiles the
20 most shootward breakpoint corresponded to the RAM/EZ boundary and the rootward breakpoint
21 corresponded to the PD/TD boundary. In 42% of cell length profiles analysed in Col-0 (17 out of
22 40 cell files), the most parsimonious model was of that of one breakpoint. This breakpoint
23 corresponded to the RAM/EZ boundary (Fig. 2C, D). We found also that for these roots the
24 second most parsimonious model was that with two breakpoints. When this model was applied,

1 the same the RAM/EZ boundary was found and additionally the PD/TD boundary was identified
2 within the RAM.

3 Similar modelling was performed for the *xall* mutant. Out of 40 cell length profiles
4 analysed, the most parsimonious model was of one, two, and three breakpoints in 30, 62, and 8%
5 of the profiles ([**Supplementary Information**, Fig. S1]. The small number of the profiles with
6 three breakpoints can represent an artefact as a consequence of greater variability in cell lengths.
7 To verify the versatility of the approach, we compared Col-0 wt with a different wt accession,
8 C24. We found that 17, 8, and 75% of cases ($n = 12$ cortical cell length profiles) showed one, two
9 and three breakpoints ([**Supplementary Information**, Table S 1].

10 Overall, our data support the existence of two developmental transitions in the growing
11 part of the root. One of these transitions, the shootward, corresponds to the RAM/EZ boundary
12 (Fig. 1A). In the next section, we will show that the second, rootward, transition corresponds to
13 the PD/TD boundary (Fig. 1B).

14

15 *The MSC modelling approach identifies the PD/TD boundary*

16 Because the different domains and root growth zones are characterized by distinct and specific
17 developmental processes, the distribution of unambiguous molecular markers for those processes
18 could also be used to define the longitudinal zonation of the root (Ivanov and Dubrovsky 2013).
19 The distribution of molecular markers for G2-to-M transition, *CycB1;I_{DB}:GUS* or
20 *CycB1;I_{DB}:GFP*, have been used as markers for the PD of the RAM (Colón-Carmona et al. 1999;
21 Hauser and Bauer 2000; Aida et al. 2004; Ticconi et al. 2004; Li et al. 2005; Cruz-Ramírez et al.
22 2012).

23 Cell length profiles were obtained from *CycB1;I_{DB}:GFP* roots grown on media with low
24 (1 mM) and high (30 mM) concentration of total nitrogen. These cell length profiles were

1 collected from assembled root images obtained under a confocal laser scanning microscope at a
2 high magnification and for this reason did not include EZ cells. *CycB1;I_{DB}:GFP* reporter detects
3 cells in late G2 and early M phases of the cell cycle (Colon-Carmona et al., 1999). Therefore, cell
4 length profile was obtained for a root portion where GFP-positive cells were detected
5 (presumptive PD) and shootward of this zone for a portion of at least half of presumptive TD.
6 Thus, if a breakpoint is detected, this should correspond to the PD/TD boundary. Roots grown on
7 the media with high and low nitrogen content differed significantly in their growth rate and
8 morphology and on medium with low nitrogen grew 2.5-fold faster than under high nitrogen
9 (Table 1). This observation suggested that the PD would be of different length in seedlings grown
10 under these contrast conditions. Indeed, the PD length determined by MSC approach was greater
11 at low nitrogen medium (Fig. 3).

12 The distribution of GFP-positive cells within the meristem was random (Fig. 3A, B). In
13 most cases, those meristematic cells that were in mitosis were GFP-positive. The cells that were
14 not in mitosis, but were weakly GFP-labelled were cells in G2 as can be deduced from their size
15 (these cells were approximately twice as long as recently divided cells). The breakpoint values
16 estimated by the MSC approach corresponded to the last PD cells. Cells that expressed
17 *CycB1;I_{DB}:GFP* at the moment of fixation were in most cases located rootward to the
18 breakpoints estimated by the MSC approach (Fig. 3C-F), i.e. within the PD domain. The
19 *CycB1;I_{DB}:GFP* expression was found in a shootward position with respect to the breakpoint
20 only in 6% of cell files analysed (5 out of 80). These data indicate that the probability of cell
21 division (GFP-positive cells) after the breakpoint estimated was low, although rapid cell
22 elongation had not yet started in the measured cell files. Our data indicate that the PD/TD
23 breakpoint estimated by MSC approach coincided well with the *CycB1;I_{DB}:GFP* expression
24 pattern.

1 As mentioned above, changes in cell proliferation are associated with the PD/TD
2 boundary before rapid elongation starts, and particularly, before the changes in elongation rates
3 can be detected, cells enter to the endoreduplication cycle (Hayashi et al. 2013). Thus, we
4 proposed that the TD can be also defined as the region where cells start endoreduplication but
5 have not yet started rapid elongation. Therefore, a molecular marker for endoreduplication, could
6 also be used to establish the PD/TD boundary. The *CELL CYCLE SWITCH52A1* (*CCS52A1*)
7 gene, an isoform of the substrate specific activator of the anaphase promoting
8 complex/cyclosome (APC/C), promotes the onset of endoreduplication and its expression
9 correlates with the transition from proliferation to endoreduplication (Vanstraelen et al. 2009).
10 The *pCCS52A1:GUS* reporter gene (Vanstraelen et al. 2009) can be used as a molecular marker
11 of the PD/TD boundary as it is expressed only in the TD and the EZ (Vanstraelen et al. 2009;
12 Takahashi et al. 2013).

13 To test if the breakpoint inside the RAM estimated by the MSC approach corresponds
14 with the transition from proliferative state to endoreduplication, we obtained the cortex cell
15 length profile of ten roots of the *pCCS52A1:GUS* reporter line. Using the MSC approach, we
16 determined the breakpoint positions for these roots and estimated 95% CI of the position of the
17 last PD cell of each cell file analysed. This position was close to the rootward (distal) border of
18 the GUS expressing region (seven out of ten cell files, or 70%) (Fig. 4A-G). In 30% of the
19 analysed cell files, the last PD cell, estimated by MSC approach was clearly in a more rootward
20 position than the GUS expressing region (Fig. 4H-J). Therefore, the PD/TD boundary estimated
21 by MSC coincided with the onset of *pCCS52A1:GUS* expression in the majority of cases.

22 These data support the conclusion that the MSC approach enabled estimation of the
23 position of PD/TD boundary and this position coincided with the distribution of cells expressing
24 the *CycB1;IDB:GFP* marker and with the onset of *pCCS52A1:GUS* expression. This PD/TD

1 transition occurred before rapid cell elongation started. Thus we conclude that there are two
2 developmental transitions in the growing part of the root: PD/TD and RAM/EZ (Fig. 1A, B), the
3 former related to changes in proliferation behaviour and the latter to the onset of rapid cell
4 elongation.

5

6 *Determination of the PD/TD boundary by MSC approach coincides with a subjective*
7 *determination by an experienced root developmental biologist*

8 In previous studies, the extension of the PD of the RAM was determined based on relative
9 changes of cell length along a root meristem cell file. The PD/TD boundary has been determined
10 at a point from the QC, where, in the shootward direction, cell length or inter-nuclear distance
11 increases significantly and where a cell becomes longer than the average cell length within the
12 PD (Dubrovsky 1997; Dubrovsky, et al. 1998a, b; Tapia-López et al. 2008; Garay-Arroyo et al.
13 2013). Blind experiments of the determination of this boundary on the same roots by different
14 biologists experienced in this technique (ExpBiol) give similar results, but students or biologists
15 that are inexperienced in this analysis obtain contrasting results (VBI, PD, and JGD, unpublished
16 observations). Therefore, the ExpBiol is subject to biases depending on the researcher that
17 conducts the analysis. Hence, we were interested in comparing ExpBiol and the MSC approaches
18 to establish the PD/TD boundary.

19 The PD/TD boundary was estimated on *CycB1;IDB::GFP* roots grown on media with low
20 (1 mM) and high (30 mM) concentration of total nitrogen. Interestingly, the PD length (estimated
21 by ExpBiol) in arabidopsis varied depending not only on the N availability, but also among roots
22 grown under the same nutrient conditions. The minimum-maximum numbers of cells in a cell file
23 within the PD (estimated by ExpBiol) in individual roots were 13-41 (epidermis), 24-48 (cortex)
24 at low N, and 9-30 (epidermis), 10-29 (cortex) at high N. Considering this variation, we analysed

1 the agreement between the PD/TD boundary estimated for each root when using the ExpBiol
2 method and the MSC approach.

3 In statistics, inter-rater reliability (IRR) indicates "the degree of agreement between two
4 or more coders who made independent ratings about the features of a set of subjects" (Hallgren
5 2012). To evaluate IRR for estimations of the number of PD cells obtained by the ExpBiol and
6 MSC approaches, we calculated the intraclass correlation coefficient (*ICC*) (McGraw and Wong
7 1996; Hallgren 2012). Higher *ICC* values indicate higher agreement. An *ICC* estimate of 1
8 indicates a perfect agreement and a 0 estimate indicates only random agreement. The *ICC*
9 estimated for all the *CycB1; I_{DB}:GFP* cell files was significantly greater than zero, $ICC = 0.9$, F
10 $(79, 80) = 10.2$, $p = 2.44e-21$, 95% CI [0.85, 0.94], and was at the excellent qualitative range
11 proposed by Cicchetti (1994), confirming that ExpBiol method (which has been traditionally
12 used) and MSC approach had a high degree of agreement as no statistical differences between the
13 two approaches were detected (Table 2). Importantly, as determined by MSC analysis, at high N
14 medium the cortex PD length was approximately 80 % shorter than that in roots grown at low N
15 medium. This indicate the versatility of the MSC approach. Given that different researchers may
16 reach different results depending on their experience, the use of MSC is recommended as it can
17 eliminate subjective estimates and provide reproducibility within and across laboratories,
18 irrespective of the experience of the observer.

19
20 *The MSC approach can be used to estimate the critical size of dividing cells and the critical cell*
21 *size for the initiation of rapid elongation*

22 Organisms, from bacteria to higher eukaryotes, coordinate cell growth and cell division through
23 size-sensing checkpoint mechanisms, in order to maintain a constant cell size. Cells have to reach
24 a certain critical size at which the cell-cycle transitions are triggered, such as G1-S or G2-mitosis

1 (Ivanov 1971; Dobrochaev and Ivanov 2001; Dolznig et al. 2004; Yang et al. 2006; Turner et al.
2 2012; Robert et al. 2014). Therefore, along the PD it is expected that cells are equal or smaller
3 than the critical size of dividing cells (L_{critD}). However, in the TD, the probability of cell division
4 is very low (Ivanov and Dubrovsky 2013); therefore, cells which continue growing at the same
5 relative growth rate as in the PD are longer than the L_{critD} (Hejnowicz 1959; Hejnowicz and
6 Brodzki 1960; Ivanov and Maximov 1999; van der Weele et al. 2003). In the EZ, rapid cell
7 elongation is taking place among other processes due to water uptake into the central vacuole
8 (reviewed by Dolan and Davies, 2004). We addressed in this study if there is a critical cell length
9 related to the onset of rapid elongation in the EZ, similar to the L_{critD} near the PD/TD boundary.
10 We denote this cell length as the critical cell size for the initiation of rapid elongation (L_{critE}).

11 To estimate the maximum cell lengths that correspond to the PD and the TD, we used the
12 MSC analysis of sorted cell lengths. We called this analysis the sorted MSC (sMSC). For this
13 procedure, we sorted cell lengths of a root cell file in ascending size order (Fig. 5A, B). Thus, cell
14 length is a function of the cell length rank in the sorted cell length set (Fig. 5B). We assumed that
15 there are three subsets of sorted cell lengths that correspond to the PD, TD and EZ. Then, after
16 estimation of the breakpoints that correspond to the ranks of the longest PD and TD cells (Fig.
17 5B, C), we found the two linear equations that model the PD and TD cell length subsets after
18 determining the breakpoints by MSC (Fig.5D). Finally, we used these two linear equations for
19 the PD and TD to estimate the maximum cell length in the PD and TD or the L_{critD} and L_{critE} ,
20 respectively (Fig. 5D). In this way the MSC approach can be used to estimate the critical size of
21 dividing cells and the critical size for the initiation of rapid elongation. These parameters were
22 subsequently used for comparison of different genotypes.

23

24 *MSC analysis of arabidopsis wt and xall roots*

1 We generated MSC models with two breakpoints for each cell length profile of wt and *xall* roots
2 at 7 and 9 DAS. From these models we estimated: (a) the position of RAM/EZ and PD/TD
3 boundaries by the MSC approach, (b) the linear equations for PD, TD and EZ, (c) the number of
4 cells and length of each domain, (d) the derivative of cell length as a function of position (DLP),
5 which corresponds to the slope of each linear equation, and (e) the L_{critD} and L_{critE} . Once the
6 PD/TD and RAM/EZ boundaries were determined by the MSC approach, we compared the sizes
7 of the RAM, PD and TD in wt and *xall* seedlings 7 and 9 DAS. We found that the number of
8 cells and length of the wt PD and RAM increased from 7 to 9 DAS (Table 3). In contrast, no
9 change was detected in the TD during this growth period in both genetic backgrounds (Table 3).
10 Thus the RAM size increase in the wt was due to a larger population of proliferating cells in the
11 PD at 9 DAS (Table 3).

12 Interestingly, in the *xall* mutant we did not detect changes in PD and RAM lengths and
13 corresponding number of cells, from 7 to 9 DAS under our growth conditions (Table 3). Because
14 an accelerated root growth is related mainly to changes in the number of proliferating cells
15 (Beemster and Baskin 1998), the almost constant growth of *xall* roots from 3 to 11 DAS (Fig.
16 6A, B) suggested that *xall* PD hardly changes at least during the first ten days. Thus, *XALI* is
17 necessary to maintain steady increase in the number of cells within the PD, and as a consequence,
18 an accelerated root growth.

19 As *xall* root cells have a longer cell cycle than wt roots (Tapia-López et al. 2008), we
20 asked if this difference is associated with a change in the L_{critD} . We estimated the mean wt cortex
21 cells (L_{critD}) as $M = 8.9 \mu\text{m}$, 95% CI [8.5, 9.3], $n = 40$, and for *xall* cortex cells as $M = 11.4 \mu\text{m}$,
22 [10.7, 12.0], $n = 40$. This suggests that the size sensing mechanism that controls the critical cell
23 size for division is altered by the loss of function of *XALI* and, as a consequence, the cell cycle
24 duration of *xall* roots is longer, because it takes more time to reach the L_{critD} (assuming the same

1 cell growth rate with respect to time). We also estimated the mean wt cortex cell critical size for
2 the initiation of rapid elongation, L_{critE} , as $M = 25 \mu\text{m}$, [23, 28], $n = 40$, and for *xal1* cortex cells
3 as $M = 38 \mu\text{m}$, [32, 44], $n = 40$. This analysis showed that, the loss of function of *XALI* altered
4 both critical sizes. In summary, the MSC analysis permitted to suggest that *XALI* may be
5 involved in the regulatory mechanisms to control critical cell size. Alternatively, *XALI*
6 expression may depend on critical cell size.

9 DISCUSSION

10 We have applied MSC model to establish the longitudinal zonation pattern of arabidopsis roots.
11 This approach is useful to estimate different parameters such as (a) the number of longitudinal
12 domains and zones, (b) the number of cells and lengths of each domains and zones, (c) cell length
13 changes with respect to cell position along the longitudinal root axis or the derivative of cell
14 length as a function of position (DLP), and (d) the critical size of dividing cells (L_{critD}), and the
15 critical size for the initiation of rapid elongation L_{critE} . Using the BIC to estimate the most
16 parsimonious models for number of breakpoints, we have detected two breakpoints or transitions
17 in cell length profiles of the growing part of the root for the majority of roots. One of these
18 breakpoints corresponds to the RAM/EZ boundary and the other one defines the PD/TD
19 boundary. When one or three breakpoints were detected as the most parsimonious, this was
20 mainly due to internal variability in cell length profiles in arabidopsis roots. Considering that (a)
21 two breakpoint model was more common; (b) one breakpoint model was a particular case where
22 the PD/TD boundary was not sharp enough; (c) *CycB1; I_{DB}:GFP* was expressed mainly in the PD
23 and (d) *pCCS52A1:GUS* was expressed mainly in the TD, we can conclude that three distinct
24 domains or zones (the PD, the TD, and the EZ) should be recognised in the arabidopsis root.

1 Some authors consider that within individual cell files there is no TD before rapid
2 elongation starts; it is viewed that the transition zone is just one point along the root where cells
3 leave the RAM and enter the EZ (see: Dello Ioio et al. 2007; Moubayidin et al. 2010). These
4 authors also consider that the onset of elongation "is different for each cell type, giving a jagged
5 shape to the boundary between dividing and expanding cells" (Dello Ioio et al. 2007, p. 679).
6 Root tissues stop dividing at different distances from the QC, but they all start rapid elongation at
7 the same distance due to symplastic growth (reviewed in Ivanov and Dubrovsky 2013). Hence,
8 before rapid elongation, the symplastic nature of plant tissues, yields a domain at which cells start
9 endoreduplication, but do not start rapid elongation; this region then corresponds to the 'TD'
10 (Baluška et al., 1996; Ivanov and Dubrovsky 2013). Indeed, experimental evidence has shown
11 that in arabidopsis endoreduplication precedes rapid cell elongation (Hayashi et al. 2013). Thus,
12 for a particular cell file within the arabidopsis root, the TD can also be defined as the region
13 where cells endoreduplicate and continue elongating at the same rate as in the PD. It has also
14 been shown that phospholipase D ζ 2, involved in vesicle trafficking, is strongly expressed in the
15 transition zone (Li and Xue, 2007; Mancuso et al. 2007).

16 The MSC analysis used here clearly shows that before the onset of rapid elongation, all
17 cells within a file, irrespective of the tissue type, are distributed in two subsets separated by an
18 identifiable transition: those in the PD and those in the TD. A clear difference between these two
19 subsets and the difference between the RAM and EZ subsets provide additional evidence that the
20 transition to elongation is not just one point along the root but comprises a domain of cells that
21 have lost or are in the process of losing proliferation activity.

22 If we consider that the RAM does not include two domains (and the transition to the EZ is
23 not considered to span several cells that constitute an identifiable domain of cells), the estimated
24 RAM linear model should have a slope or DLP greater than zero. This would imply then that

1 along the RAM, the relative cell elongation rate is greater than the relative cell division rate, but
2 cell length profiles do not show a cell length distribution that corresponds to this scenario (Fig.
3 2). Within each domain, different relationships between relative elongation and cell division rates
4 (Green 1976) or DLPs cause a change in the mean cell length. We have found that on average the
5 PD DLP is equal to zero and the TD DLP is greater than zero (Table 3). This implies that in the
6 PD there is a balance between relative cell elongation and division rates (Baskin, 2000), while in
7 the TD relative elongation rates are greater than relative division rates. So, our results support the
8 existence of two domains within the RAM. Thus, cell length profiles that include the RAM and
9 the EZ must be modelled by two breakpoints MSC models.

10 The PD/TD boundary is difficult to recognize, partially because relative changes in cell
11 lengths, which not always steadily increase in shootward direction, have to be evaluated. Using a
12 molecular marker such as *CycB1;IDB::GFP* we found here, that most of GFP expressing cells
13 were within the PD defined by the MSC approach. However, the fact that in 6% of cases GFP
14 expressing cells were found in the TD, indicate two important aspects: (a) that some TD cells
15 indeed are able to proliferate and (b) that an estimation error must be considered. This same
16 conclusion can be drawn to explain why in some cases *pGUS::CCS52A1* expression is detected
17 shootward of the MSC-determined position of the PD/TD boundary (Fig. 4H-J). Additionally,
18 this discrepancy can be explained by the observation that in arabidopsis roots, the
19 endoreduplication cycle can also start in the EZ and that its duration is greater than that of the cell
20 cycle in the RAM (Hayashi et al., 2013).

21 It is important to point out that the cells at the TD have unique physiological properties
22 such as alterations in their cell-wall structure and the onset of vacuolization that enables fast cell
23 growth at the EZ (Verbelen et al. 2006; Baluška et al. 2010). It has also been described that cells
24 in the TD are very sensitive to diverse external factors such as gravity, light, oxidative stress and

1 humidity (Verbelen et al. 2006). Thus, evaluating the extent to which such domain is altered
2 under different genetic and environmental conditions, becomes very relevant. In this paper, we
3 propose an approach to objectively establish the boundaries between the PD and the TD, and
4 between the RAM and the EZ, as well as the sizes and number of cells comprising each domain.

5 Using MSC, we have found that the PD in wt roots increases after 7 DAS, and such
6 growth is related to an increase in the number of proliferating cells and accelerated root growth,
7 after 7 DAS. This observation is in accordance with many studies where similar criteria to
8 determine the RAM/EZ boundary have been used, and which report meristem length increase
9 after 5 days after germination (DAG) and later (Galinha et al. 2007; Ubeda-Tomás et al. 2009;
10 González-García et al. 2011; Makkena and Lamb 2013). Moreover, a kinematic analysis of the
11 arabidopsis root showed that accelerated root growth is mainly due to an increased cell
12 production rate during the first 14 DAG, and a steady increase in meristem length during the first
13 two weeks of growth after germination (Beemster and Baskin 1998). These results are similar to
14 our observations of accelerated growth from 7 to 11 DAS (Fig. 6A, B), accompanied with an
15 increase in the PD length. However, these results contrast with some previous studies that
16 concluded that wt arabidopsis RAM reaches its maximum size 5 DAG (Dello Ioio et al. 2007;
17 Achard et al. 2009; Moubayidin et al. 2010; Zhou et al. 2011), equivalent to our 7 DAS. This
18 discrepancy about the age at which the RAM reaches its maximum size can be explained by the
19 fact that this age is highly dependent on environmental conditions that vary among studies and by
20 possible methodological differences in meristem length determination. In any case, these
21 variations among laboratories highlight the need for a reliable approach to identify root growth
22 zones along its longitudinal axis and their boundaries. In contrast, *xal1* roots showed an almost
23 constant root growth rate (Fig. 6A, B), possibly because the PD length hardly changes during, at

1 least, 7 to 10 DAS. This result suggests that *XALI* is involved in the regulation of the transition
2 from the PD to the TD.

3 Interestingly, the L_{critD} is altered by the loss of function of *XALI*, suggesting that the
4 longer cell cycle duration estimated in *xall* roots (Tapia-López et al. 2008) is possibly related to
5 alterations in the size sensing mechanisms that control the onset of cell division. Fully elongated
6 cells of *xall* roots are shorter on average than wt ones (Tapia-López et al. 2008). Nonetheless,
7 our results show that cells that enter the EZ are larger in *xall* roots than in wt. Then, cell
8 elongation stops at shorter cell lengths in *xall* than in wt roots, although *xall* cells initiate rapid
9 cell elongation at larger sizes. Our results suggest that the loss of function of *XALI* alter the two
10 developmental transitions along the root (PD/TD and RAM/EZ), as well as cell critical sizes.
11 Future studies will have to unravel how *XALI* is involved in the regulation of cell division rate,
12 directly or indirectly, through the regulation of the mechanisms that control the L_{critD} .

13 In conclusion, the MSC approach for determination of the PD/TD boundary yields similar
14 results to those based on specific molecular markers and those obtained by the ExpBiol
15 subjective method. The MSC approach is an objective and versatile tool for determination of
16 domains and zones and gives reliable results for roots with the RAM of different lengths. The use
17 of molecular markers implies genetic crosses and frequently, mixture of different genetic
18 backgrounds. To avoid this problem, the MSC approach permits a direct longitudinal zonation
19 pattern characterisation. It can be used for different genetic backgrounds, treatments, or can be
20 applied for analysis of developmental changes taking place with age. This approach potentially
21 could also be applied to species other than arabidopsis to better characterize and understand the
22 mechanisms underlying the homeostasis of the RAM in Angiosperms.

23

24

SUPPLEMENTARY INFORMATION

1 Supplementary information is available online at www.aob.oxford-journals.org and consists of
2 the following:
3 Text S1: Instructions to analyse a cell length profile of arabidopsis root using the ‘strucchange’
4 package of R (two examples).
5 Figure S1. Estimation of the number of breakpoints and their position by a MSC-BIC approach in
6 *xall* 9DAS seedling.
7 Table S1. Quantitative analysis of Arabidopsis C24 wild-type (wt) roots
8
9

10

11

ACKNOWLEDGMENTS

12

13

14

15

16

17

18

19

20

21

22

23

24

25

We thank the [Arabidopsis Biological Resource Center](#) at the Ohio State University for arabidopsis wild type seeds, Eva Kondorosi for providing *pCCS52A1:GUS* line. We also thank Diana Romo who helped with logistical and laboratory tasks, to Marcela Ramírez-Yarza for technical help, graphic designer Francisco José Guijarro Higuera for the root micrograph collage of Fig. 1 and Natalia Doktor for help in confocal microscopy image assemblage and preparation of Fig. 3. The support of B. García Ponce (BGP) de León and MP Sánchez Jiménez (MPSJ) is acknowledged. This work was supported by Consejo Nacional de Ciencia y Tecnología, CONACyT, [180098 and 180380 to ERAB, 167705 to AGA, 152649 to MPSJ, 237430 and 206843 to JGD]; UNAM-DGAPA-PAPIIT [IN203113 to ERAB, IN204011 to BGP, IN226510-3 to AGA, IN203814 to MPSJ and IN205315 to JGD]; Mexican Academy of Sciences and The Royal Society, UK to JGD and PD; and Russian Foundation for Basic Research [Grant RFBR-15-04-02502a to VBI and IAB]. This work represents a partial fulfilment of the requirements of the PhD of MAPE at the Posgrado en Ciencias Biomédicas, Universidad Nacional Autónoma de México. Financial support for MAPE was provided by the Ph.D. grant program of CONACyT.

1

2

LITERATURE CITED

3 **Achard P, Gusti A, Cheminant S, Alioua M, Dhondt S, Coppens F, Beemster GTS,**
4 **Genschik P. 2009.** Gibberellin signaling controls cell proliferation rate in Arabidopsis. *Current*
5 *biology* **19**: 1188–93.

6 **Aida M, Beis D, Heidstra R, Willemsen V. 2004.** The PLETHORA genes mediate patterning of
7 the *Arabidopsis* root stem cell niche. *Cell* **119**: 109–120.

8 **Auger IE, Lawrence CE. 1989.** Algorithms for the optimal identification of segmented
9 neighborhoods. *Bulletin of Mathematical Biology* **51**: 39–54.

10 **Bai J. 1997.** Estimation of a change point in multiple regression models. *Review of Economics*
11 *and Statistics* **79**: 551–563.

12 **Bai J, Perron P. 1998.** Estimating and Testing Linear Models with Multiple Structural Changes.
13 *Econometrica* **66**: 47–78.

14 **Bai J, Perron P. 2003.** Computation and analysis of multiple structural change models. *Journal*
15 *of Applied Econometrics* **18**: 1–22.

16 **Baluška F, Mancuso S. 2013.** Root apex transition zone as oscillatory zone. *Frontiers in plant*
17 *science* **4**: 354.

18 **Baluška F, Mancuso S, Volkmann D, Barlow PW. 2010.** Root apex transition zone: A
19 signalling-response nexus in the root. *Trends in Plant Science* **15**: 402–408.

20 **Baluška F, Volkmann D, Barlow PW. 1996.** Specialized zones of development in roots: view
21 from the cellular level. *Plant Physiology* **112**: 3-4.

22 **Baskin TI. 2000.** On the constancy of cell division rate in the root meristem. *Plant molecular*
23 *biology* **43**: 545–54.

24 **Beemster GT, Baskin TI. 1998.** Analysis of cell division and elongation underlying the
25 developmental acceleration of root growth in *Arabidopsis thaliana*. *Plant Physiology* **116**: 1515–
26 26.

27 **Casamitjana-Martínez E, Hofhuis HF, Xu J, Liu C-M, Heidstra R, Scheres B. 2003.** Root-
28 specific CLE19 overexpression and the *sol1/2* suppressors implicate a CLV-like pathway in the
29 control of *Arabidopsis* root meristem maintenance. *Current biology* : **CB 13**: 1435–41.

30 **Cicchetti D V. 1994.** Guidelines, criteria, and rules of thumb for evaluating normed and
31 standardized assessment instruments in psychology. *Psychological Assessment* **6**: 284–290.

- 1 **Clowes FAL. 1956.** Nucleic acids in root apical meristems of *Zea*. *New Phytologist* **55**: 29–34.
- 2 **Colón-Carmona A, You R, Haimovitch-Gal T, Doerner P. 1999.** Spatio-temporal analysis of
3 mitotic activity with a labile cyclin-GUS fusion protein. *Plant Journal* **20**: 503–508.
- 4 **Cruz-Ramírez A, Díaz-Triviño S, Blilou I, Grieneisen V a, Sozzani R, Zamioudis C,**
5 **Miskolczi P, Nieuwland J, Benjamins R, Dhonukshe P, Caballero-Pérez J, Horvath B, Long**
6 **Y, Mähönen AP, Zhang H, Xu J, Murray J a H, Benfey PN, Bako L, Marée AFM, Scheres**
7 **B. 2012.** A bistable circuit involving SCARECROW-RETINOBLASTOMA integrates cues to
8 inform asymmetric stem cell division. *Cell* **150**: 1002–15.
- 9 **Dobrochaev AE, Ivanov VB. 2001.** Variations in the size of mitotic cells in the root meristem.
10 *Ontogenez* **32**: 252–62.
- 11 **Dolan L, Davies J. 2004.** Cell expansion in roots. *Current Opinion in Plant Biology* **7**: 33–39.
- 12 **Dolan L, Janmaat K, Willemsen V, Linstead P, Poethig S, Roberts K, Scheres B. 1993.**
13 Cellular organisation of the *Arabidopsis thaliana* root. *Development* **119**: 71–84.
- 14 **Dolznic H, Grebien F, Sauer T, Beug H, Müllner EW. 2004.** Evidence for a size-sensing
15 mechanism in animal cells. *Nature cell biology* **6**: 899–905.
- 16 **Dubrovsky JG. 1997.** Determinate primary-root growth in seedlings of Sonoran Desert
17 Cactaceae; its organization, cellular basis, and ecological significance. *Planta* **203**: 85–92.
- 18 **Dubrovsky J, Contreras-Burciaga L, Ivanov VB. 1998a.** Cell cycle duration in the root
19 meristem of Sonoran Desert Cactaceae as estimated by cell-flow and rate-of-cell-production
20 methods. *Annals of Botany* **81**: 619–624.
- 21 **Dubrovsky J, North G, Nobel P. 1998b.** Root growth, developmental changes in the apex, and
22 hydraulic conductivity for *Opuntia ficus-indica* during drought. *New Phytologist* **138**: 75–82.
- 23 **French AP, Wilson MH, Kenobi K, Dietrich D, Voß U, Ubeda-Tomás S, Pridmore TP,**
24 **Wells DM. 2012.** Identifying biological landmarks using a novel cell measuring image analysis
25 tool: Cell-o-Tape. *Plant methods* **8**: 7.
- 26 **Galinha C, Hofhuis H, Luijten M, Willemsen V, Blilou I, Heidstra R, Scheres B. 2007.**
27 PLETHORA proteins as dose-dependent master regulators of *Arabidopsis* root development.
28 *Nature* **449**: 1053–7.
- 29 **Garay-Arroyo A, Ortiz-Moreno E, de la Paz Sánchez M, Murphy AS, García-Ponce B,**
30 **Marsch-Martínez N, de Folter S, Corvera-Poiré A, Jaimes-Miranda F, Pacheco-Escobedo**
31 **MA, Dubrovsky JG, Pelaz S, Alvarez-Buylla ER. 2013.** The MADS transcription factor
32 XAL2/AGL14 modulates auxin transport during *Arabidopsis* root development by regulating PIN
33 expression. *The EMBO journal* **32**: 2884–95.

- 1 **González-García M-P, Vilarrasa-Blasi J, Zhiponova M, Divol F, Mora-García S, Russinova**
2 **E, Caño-Delgado AI. 2011.** Brassinosteroids control meristem size by promoting cell cycle
3 progression in Arabidopsis roots. *Development* **138**: 849–59.
- 4 **Green PB. 1976.** Growth and cell pattern formation on an axis: critique of concepts,
5 terminology, and modes of study. *Botanical Gazette* **137**: 187–202.
- 6 **Hallgren K. 2012.** Computing inter-rater reliability for observational data: An overview and
7 tutorial. *Tutorials in quantitative methods for psychology* **8**: 23–34.
- 8 **Hauser MT, Bauer E. 2000.** Histochemical analysis of root meristem activity in Arabidopsis
9 thaliana using a cyclin: GUS (β -glucuronidase) marker line. *Plant and Soil* **226**: 1–10.
- 10 **Hayashi K, Hasegawa J, Matsunaga S. 2013.** The boundary of the meristematic and elongation
11 zones in roots: endoreduplication precedes rapid cell expansion. *Scientific reports* **3**: 2723.
- 12 **Hejnowicz Z. 1959.** Growth and cell division in the apical meristem of wheat roots. *Physiologia*
13 *Plantarum* **12**: 124–138.
- 14 **Hejnowicz Z, Brodzki VY. 1960.** The growth of root cells as the function of time and their
15 position in the root. *Acta Soc.Bot.Pol* **29**: 625–644.
- 16 **Herr Jr JM. 1971.** A New Clearing-Squash Technique for the Study of Ovule Development in
17 Angiosperms. *American journal of Botany* **58**: 785–790.
- 18 **Dello Ioio R, Linhares FS, Scacchi E, Casamitjana-Martinez E, Heidstra R, Costantino P,**
19 **Sabatini S. 2007.** Cytokinins determine Arabidopsis root-meristem size by controlling cell
20 differentiation. *Current biology* **17**: 678–82.
- 21 **Ivanov VB. 1971.** Critical Size and Transition of cell to Division. Successive Transition of Sister
22 Cells to Mitosis and Obligatory Transition of Cell to Mitosis in the Root Tip of Maize Germling.
23 *Ontogenez* **2**: 524–535.
- 24 **Ivanov VB, Dubrovsky JG. 2013.** Longitudinal zonation pattern in plant roots: conflicts and
25 solutions. *Trends in plant science* **18**: 237–243.
- 26 **Ivanov VB, Maximov VN. 1999.** The change in the relative rate of cell elongation along the root
27 meristem and the apical region of the elongation zone. *Russian Journal of Plant Physiology* **46**:
28 73–82.
- 29 **Kim H-J, Fay MP, Feuer EJ, Midthune DN. 2000.** Permutation tests for joinpoint regression
30 with applications to cancer rates. *Statistics in Medicine* **19**: 335–351.
- 31 **Kim H-J, Yu B, Feuer EJ. 2009.** Selecting the Number of Change-Points in Segmented Line
32 Regression. *Statistica Sinica* **19**: 597–609.
- 33 **Li C, Potuschak T, Colón-Carmona A, Gutiérrez RA, Doerner P. 2005.** Arabidopsis TCP20

1 links regulation of growth and cell division control pathways. *Proceedings of the National*
2 *Academy of Sciences of the United States of America* **102**: 12978–12983.

3 **Li G, Xue H-W. 2007.** *Arabidopsis* PLD ζ 2 regulates vesicle trafficking and is required for auxin
4 response. *Plant Cell* **19**: 281-295.

5 **Liu J, Wu S, Zidek J V. 1997.** On Segmented Multivariate Regression. *Statistica Sinica* **7**: 497–
6 525.

7 **Ma Z, Baskin TI, Brown KM, Lynch JP. 2003.** Regulation of root elongation under
8 phosphorus stress involves changes in ethylene responsiveness. *Plant physiology* **131**: 1381–
9 1390.

10 **Makkena S, Lamb RS. 2013.** The bHLH transcription factor SPATULA regulates root growth
11 by controlling the size of the root meristem. *BMC plant biology* **13**: 1.

12 **Malamy JE, Benfey PN. 1997.** Organization and cell differentiation in lateral roots of
13 *Arabidopsis thaliana*. *Development* **124**: 33–44.

14 **Mancuso S, Marras AM, Mugnai S, Schlicht M, Zarsky V, Li G, Song L, Hue HW, Baluška**
15 **F. 2007.** Phospholipase D ζ 2 drives vesicular secretion of auxin for its polar cell-cell transport in
16 the transition zone of the root apex. *Plant Signaling & Behavior* **2**: 240-244.

17 **Matthias G, Jim L, Ian F, Puspendra S. 2012.** irr: Various Coefficients of Interrater Reliability
18 and Agreement.

19 **McGraw KO, Wong SP. 1996.** Forming inferences about some intraclass correlation
20 coefficients. *Psychological Methods* **1**: 30–46.

21 **Moubayidin L, Perilli S, Dello Ioio R, Di Mambro R, Costantino P, Sabatini S. 2010.** The
22 rate of cell differentiation controls the *Arabidopsis* root meristem growth phase. *Current biology*
23 **20**: 1138–43.

24 **Muggeo VMR. 2003.** Estimating regression models with unknown break-points. *Statistics in*
25 *Medicine* **22**: 3055–3071.

26 **Robert L, Hoffmann M, Krell N, Aymerich S, Robert J, Doumic M. 2014.** Division in
27 *Escherichia coli* is triggered by a size-sensing rather than a timing mechanism. *BMC biology* **12**:
28 17.

29 **Rost T, Baum S. 1988.** On the correlation of primary root length, meristem size and protoxylem
30 tracheary element position in pea seedlings. *American journal of botany* **75**: 414–424.

31 **Sabatini S, Heidstra R, Wildwater M, Scheres B. 2003.** SCARECROW is involved in
32 positioning the stem cell niche in the *Arabidopsis* root meristem. *Genes & development* **17**: 354–
33 8.

- 1 **Silk WK, Hsiao TC, Diederhoben U, Matson C. 1986.** Spatial distributions of potassium,
2 solutes, and their deposition rates in the growth zone of the primary corn root. *Plant physiology*
3 **82:** 853–858.
- 4 **Takahashi N, Kajihara T, Okamura C, Kim Y, Katagiri Y, Okushima Y, Matsunaga S,**
5 **Hwang I, Umeda M. 2013.** Cytokinins control endocycle onset by promoting the expression of
6 an APC/C activator in Arabidopsis roots. *Current biology* **23:** 1812–7.
- 7 **Tapia-López R, García-Ponce B, Dubrovsky JG, Garay-Arroyo A, Pérez-Ruiz R V, Kim S-**
8 **H, Acevedo F, Pelaz S, Alvarez-Buylla ER. 2008.** An AGAMOUS-related MADS-box gene,
9 XAL1 (AGL12), regulates root meristem cell proliferation and flowering transition in
10 Arabidopsis. *Plant physiology* **146:** 1182–92.
- 11 **Ticconi CA, Delatorre CA, Lahner B, Salt DE, Abel S. 2004.** Arabidopsis pdr2 reveals a
12 phosphate-sensitive checkpoint in root development. *Plant Journal* **37:** 801–814.
- 13 **Tsukagoshi H, Busch W, Benfey PN. 2010.** Transcriptional regulation of ROS controls
14 transition from proliferation to differentiation in the root. *Cell* **143:** 606–16.
- 15 **Turner JJ, Ewald JC, Skotheim JM. 2012.** Cell Size Control in Yeast. *Current Biology* **22:**
16 R350–R359.
- 17 **Ubeda-Tomás S, Federici F, Casimiro I, Beemster GTS, Bhalerao R, Swarup R, Doerner P,**
18 **Haseloff J, Bennett MJ. 2009.** Gibberellin signaling in the endodermis controls Arabidopsis root
19 meristem size. *Current biology* **19:** 1194–9.
- 20 **Vanstraelen M, Baloban M, Da Ines O, Cultrone A, Lammens T, Boudolf V, Brown SC, De**
21 **Veylder L, Mergaert P, Kondorosi E. 2009.** APC/C-CCS52A complexes control meristem
22 maintenance in the Arabidopsis root. *Proceedings of the National Academy of Sciences of the*
23 *United States of America* **106:** 11806–11.
- 24 **Verbelen J-P, De Cnodder T, Le J, Vissenberg K, Baluška F. 2006.** The Root Apex of
25 Arabidopsis thaliana Consists of Four Distinct Zones of Growth Activities: Meristematic Zone,
26 Transition Zone, Fast Elongation Zone and Growth Terminating Zone. *Plant signaling &*
27 *behavior* **1:** 296–304.
- 28 **van der Weele C, Jiang H, Palaniappan K, Ivanov V, Palaniappan K, Baskin T. 2003.** A
29 New Algorithm for Computational Image Analysis of Deformable Motion at High Spatial and
30 Temporal Resolution Applied to Root Growth. Roughly Uniform Elongation in the Meristem and
31 Also, after an Abrupt Acceleration, in the Elongation Zone. *Plant Physiology* **132:** 1138–1148.
- 32 **Yang L, Han Z, MacLellan WR, Weiss JN, Qu Z. 2006.** Linking cell division to cell growth in
33 a spatiotemporal model of the cell cycle. *Journal of theoretical biology* **241:** 120–133.
- 34 **Yao Y-C. 1988.** Estimating the number of change-points via Schwarz' criterion. *Statistics &*

- 1 *Probability Letters* **6**: 181–189.
- 2 **Zeileis A, Kleiber C, Walter K, Hornik K. 2003.** Testing and dating of structural changes in
3 practice. *Computational Statistics and Data Analysis* **44**: 109–123.
- 4 **Zeileis A, Leisch F, Hornik K, Kleiber C. 2002.** strucchange: an R package for testing for
5 structural change in linear regression models. *Journal of Statistical Software* **7**: 1–38.
- 6 **Zhou X, Li Q, Chen X, Liu J, Zhang Q, Liu Y, Liu K, Xu J. 2011.** The Arabidopsis
7 RETARDED ROOT GROWTH gene encodes a mitochondria-localized protein that is required
8 for cell division in the root meristem. *Plant physiology* **157**: 1793–804.
- 9

1 TABLE 1. *Root growth and meristem characteristics in 7 days after sowing (DAS) seedlings of*
 2 *CycB1;1_{DB}:GFP (BJ3) line grown in the media with low and high concentrations of total*
 3 *Nitrogen*

		Low Nitrogen		High Nitrogen	
		Mean (sd) (n)	95% CI	Mean (sd) (n)	95% CI
Root length (mm)		43.2 (6.9) (47)	[41.2, 45.2]	20.7 (5.3) (44)	[19.1, 22.3]
Rate of root growth during last 24 h ($\mu\text{m h}^{-1}$)		400 (137) (47)	[360, 440]	160 (66) (44)	[140, 180]
Root thickness (μm)		146 (11) (29)	[142, 150]	123 (12) (36)	[119, 127]
Fraction of GFP positive cells per cell file (%)	Epidermis	12.6 (7.5) (39)	[10.2, 15.0]	12.1 (9.8) (57)	[9.5, 14.7]
	Cortex	11.7 (7.7) (35)	[9.1, 14.3]	13.9 (9.8) (43)	[10.9, 16.9]

4
5
6
7
8
9
10
11
12
13

1 TABLE 2. *Agreement between determinations of the PD/TD boundary by ExpBiol method and by*
 2 *the MSC approach in roots of CycB1;1_{DB}:GFP (BJ3) line (n=20).*

	Distance from the PD/TD boundary to QC (μm)				Number of PD cells			
	ExpBiol		MSC		ExpBiol		MSC	
	Mean (sd)	95% CI	Mean (sd)	95% CI	Mean (sd)	95% CI	Mean (sd)	95% CI
Epidermis low N	247 (37)	[229, 264]	241 (47)	[218, 263]	28 (10)	[24, 33]	27 (9)	[23, 31]
Epidermis high N	199 (20)	[190, 209]	204 (57)	[178, 231]	18 (4)	[16, 20]	18 (5)	[16, 21]
Cortex low N	245 (38)	[227, 262]	270 (54)	[245, 295]	33 (6)	[30, 36]	36 (6)	[33, 39]
Cortex high N	195 (23)	[185, 206]	211 (40)	[192, 229]	22 (4)	[20, 24]	23 (5)	[21, 26]

3
 4
 5
 6
 7
 8
 9
 10
 11
 12
 13
 14
 15
 16
 17

1 TABLE 3. *Quantitative analysis of Arabidopsis Col-0 wild-type (wt) and xall roots, evaluated at 7*
 2 *and 9 days after sowing (DAS) by MSC analysis, (n = 20).*

	wt				<i>xall</i>			
	7 DAS		9 DAS		7 DAS		9 DAS	
	Mean (sd)	95% CI	Mean (sd)	95% CI	Mean (sd)	95% CI	Mean (sd)	95% CI
Number PD cells	40 (7)	[36, 43]	49 (6)	[46, 52]	26 (6)	[23, 28]	28 (7)	[24, 31]
Number RAM cells	55 (5)	[52, 57]	63(5)	[60, 65]	36 (5)	[34, 38]	39 (5)	[36, 41]
PD length (µm)	245 (53)	[220, 270]	316 (53)	[291, 340]	189 (63)	[160, 218]	210 (63)	[181, 240]
TD length (µm)	215 (56)	[188, 241]	216 (56)	[189, 242]	216 (121)	[160, 273]	206 (78)	[170, 243]
RAM length (µm)	460 (61)	[431, 488]	531 (45)	[510, 552]	405 (145)	[337, 473]	417 (90)	[375, 459]
PD DLP (µm/ cell position)	0.0 (0.1)	[-0.04, 0.04]	0.0 (0.1)	[0.0, 0.1]	0.1 (0.2)	[0.0, 0.1]	0.1 (0.2)	[0.0, 0.1]
TD DLP (µm/ cell position)	1.5 (1)	[0.8, 2.1]	1.3 (1)	[1.1, 1.6]	2.7 (3.1)	[1.2, 4.1]	2.6 (2.2)	[1.5, 3.6]
EZ DLP (µm/cell position)	13 (4)	[11, 15]	11 (3)	[10, 12]	13 (11)	[8, 18]	15 (6)	[12, 18]
Rank of the <i>L_{critD}</i>	43 (4)	[41,45]	50 (5)	[48, 53]	29 (4)	[27, 31]	30 (5)	[28, 32]
Rank of the <i>L_{critE}</i>	55 (5)	[52, 57]	63 (5)	[60, 65]	37 (4)	[35, 39]	38 (5)	[36, 41]

3
4
5
6
7
8
9

FIGURE LEGENDS

1
2
3
4
5
6
7
8
9
10
11
12
13
14
15
16
17
18
19
20
21
22
23
24

Fig. 1. Anatomical topology of the arabidopsis root. (A) The Root apical meristem (RAM) and Elongation Zone (EZ) of a wild type arabidopsis Col-0 seedling root, 7 days after sowing; composed image from a cleared root preparation. (B) RAM of the same root shown in (A). The numbers represent the cell position with respect to the QC (zero position). The n position corresponds to the first cortex cell adjacent to an epidermal cell that started to form a root hair bulge. Scale bars = 100 μ m.

Fig. 2. Estimation of the number of breakpoints and their position by a MSC-BIC approach in Col-0 wild type cortical cell length profiles. (A and C) MSC-BIC models with m breakpoints for representative cell length profiles shown on (B) and (D). The lowest value of BIC corresponds to the most parsimonious model for number of breakpoints within a cell file. (B and D) Representative cell length profiles of wt of 9 DAS seedlings. Vertical dashed lines represent the breakpoint position estimated by a MSC approach.

Fig. 3. Distribution pattern of *CycB1;I_{DB}:GFP* expression used as a molecular marker for the PD determination and comparison of the PD/TD border determinations by the ExpBiol and MSC approach. (A and B) Root tip longitudinal median sections made with aid of the laser scanning confocal microscopy. GFP and DAPI channels were merged and images taken at different level from the root tip were assembled; GFP signal is pseudo-coloured as magenta. (A) Roots grown on medium with 1mM of N. (B) Roots grown at medium with 30 mM of N. Yellow arrows indicate the PD/TD boundary for cortex and epidermis files determined by ExpBiol based on the changes in the cell lengths or the inter-nuclear distance; green arrows indicate the location within the PD where the cell expresses *CycB1;I_{DB}:GFP* and is closest to the PD/TD boundary in an

1 epidermis (E) or cortex (C) files; white arrows indicate the PD/TD boundary determined by the
2 MSC approach. Scale bar = 50 μm . (C-F) X-axis numbers indicate different cell files analysed (n
3 = 10 roots, one file of cortex and one file of epidermis for each root). The position of the last PD
4 cell determined by MSC approach (black dots) and the position of the cells closest to the PD/TD
5 boundary which expresses GFP (asterisks) in epidermis and cortex files for the low and high
6 nitrogen media are shown. Note that not each cell file had cells expressing *CycB1;1_{DB}:GFP* at
7 moment of fixation. For each condition cell files are arranged in an ascending order of the
8 number of cells in the PD determined by MSC approach.

9
10 Fig. 4. Determination of the PD/TD boundary in *CCS52A1:GUS* line using the MSC approach;
11 *GUS* expression marks the beginning of endoreduplication. (A-J) *CCS52A1:GUS* expression in
12 wt roots (7 DAS) occurs in the TD and EZ. Yellow rectangles indicate the 95% CI of the position
13 of the last PD cell estimated by the MSC approach. Scale bar = 50 μm .

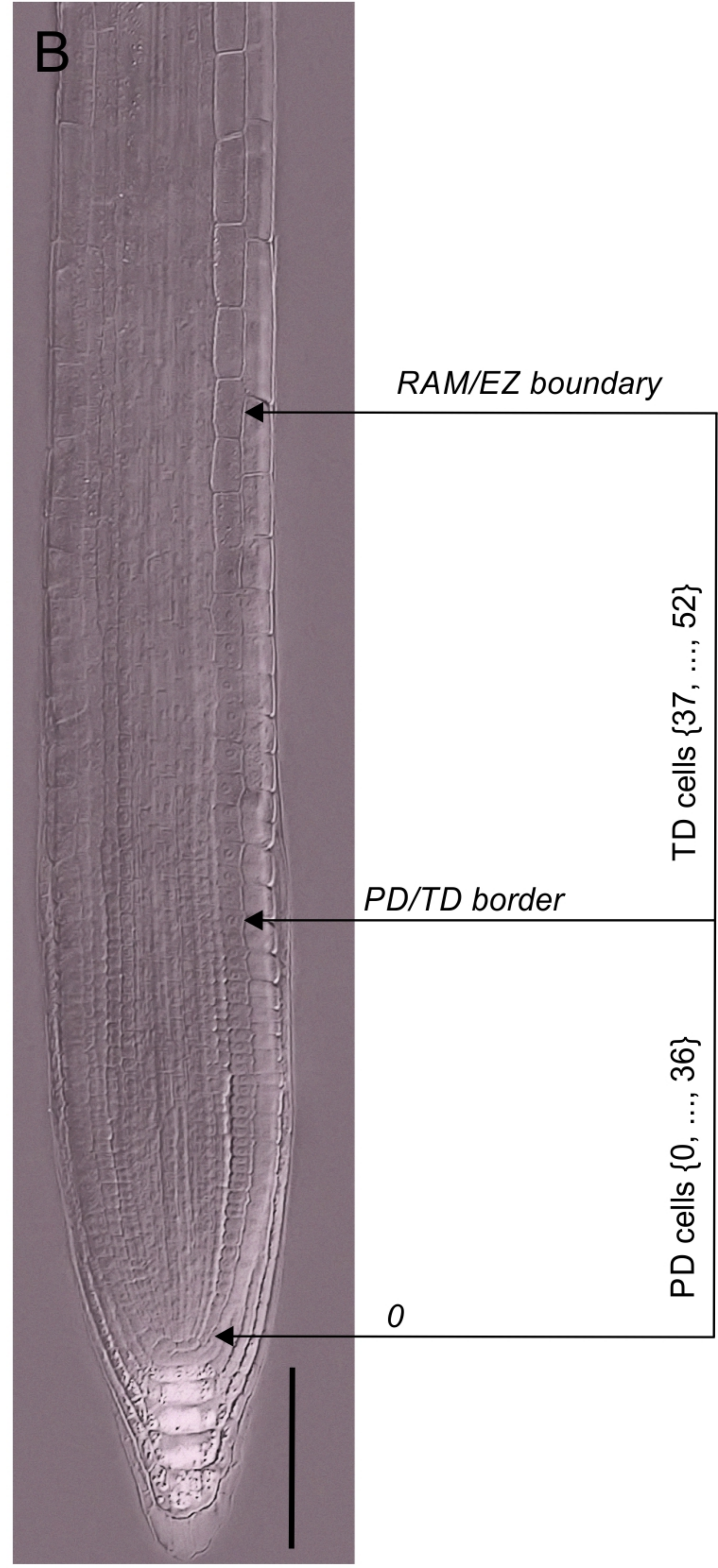
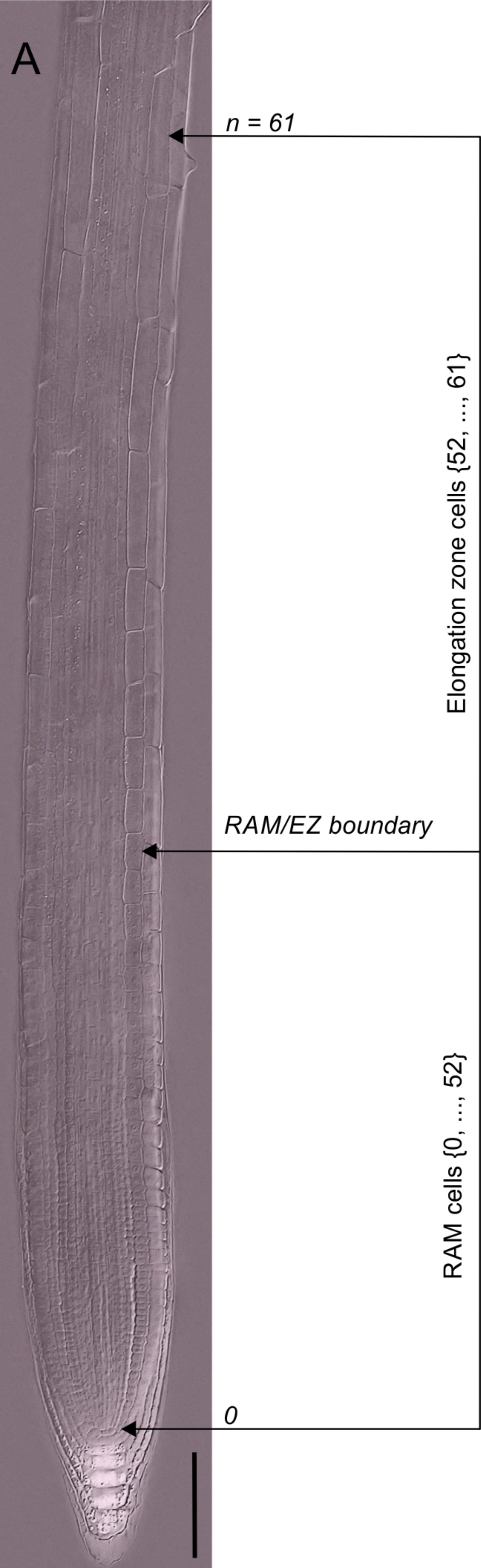
14
15 Fig. 5. Estimation of the critical size of dividing and elongating cells by sMSC approach. (A)
16 Cortex cell length profile of the growing part of a representative root of wt Col-0, nine days after
17 sowing. (B) Sorted cell length profile in ascending order of the growing part of the same root
18 shown in (A). Vertical dashed lines represent positions of breakpoints, estimated by the MSC
19 approach, that correspond to the PD/ TD and the RAM/EZ boundaries of sorted cell lengths. (C)
20 Sorted RAM cell length profile of the RAM of the root shown in (A) and (B). Vertical dashed
21 line represents the breakpoint that delimitates the PD and TD cell length sets. (D) Linear models
22 for PD and TD cell length sets. Black dot represents the estimated critical size of dividing cells
23 (L_{critD}) and white triangle represents the critical size for the initiation of rapid elongation (L_{critE})
24 for the file of the cortex shown in (A).

1

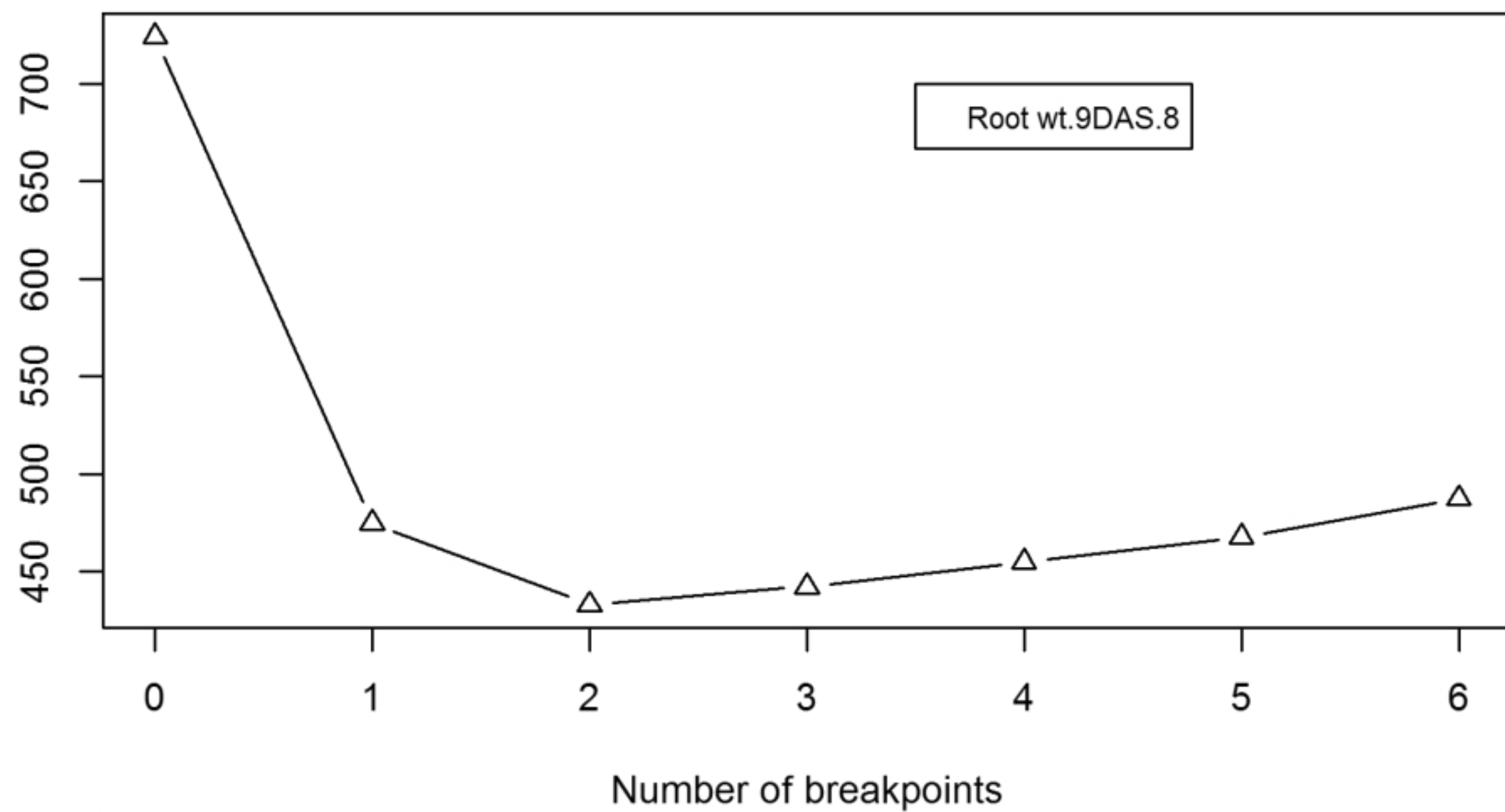
2 Fig. 6. Growth of wt and *xall* roots. (A) Root growth dynamics in wt (white circles) and *xall*

3 (black dots) roots. (B) Root growth rates over time in wt (white circles) and *xall* (black dots).

4 Error bars represent 95% CI, $n = 20$.

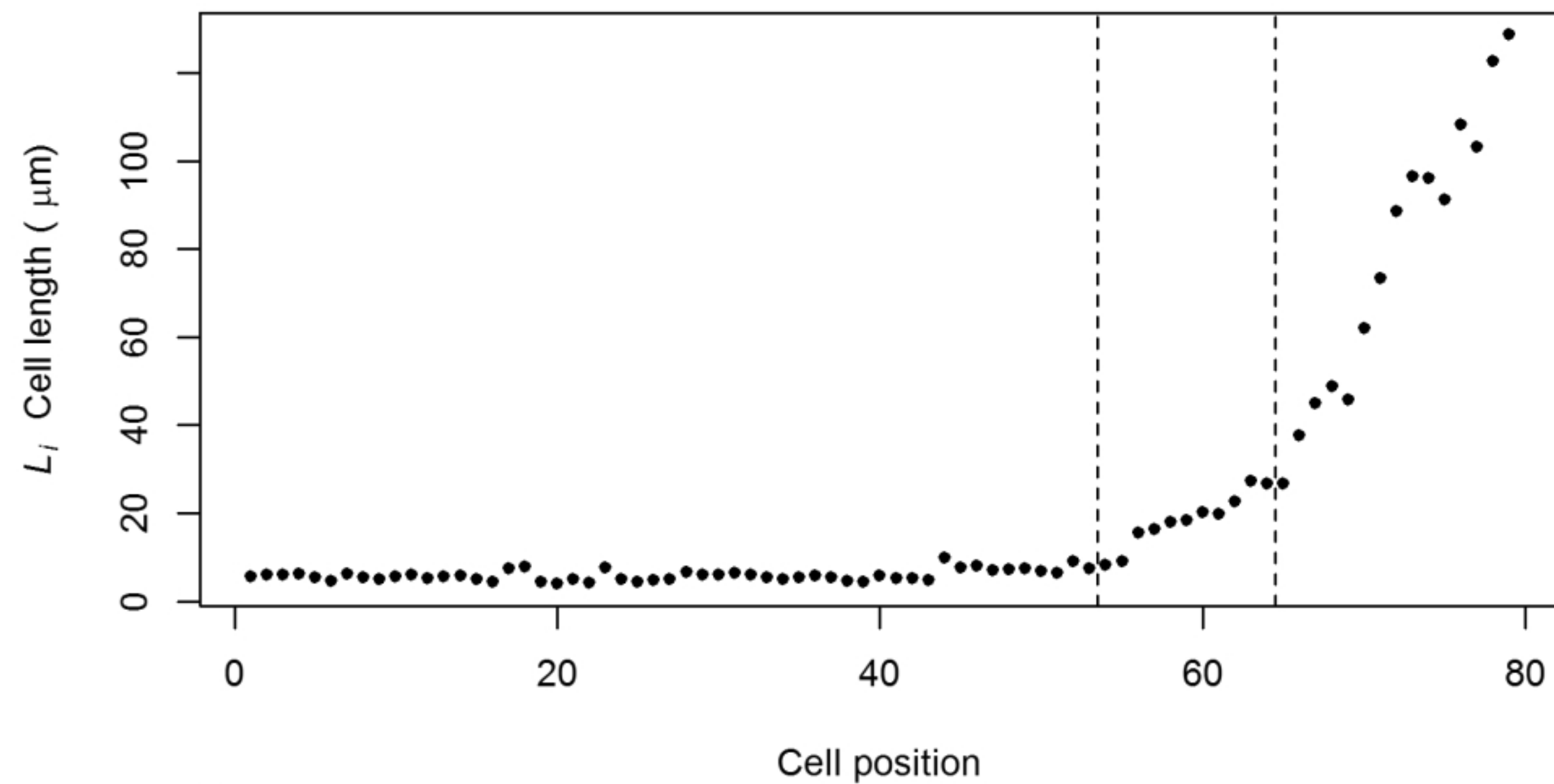


A

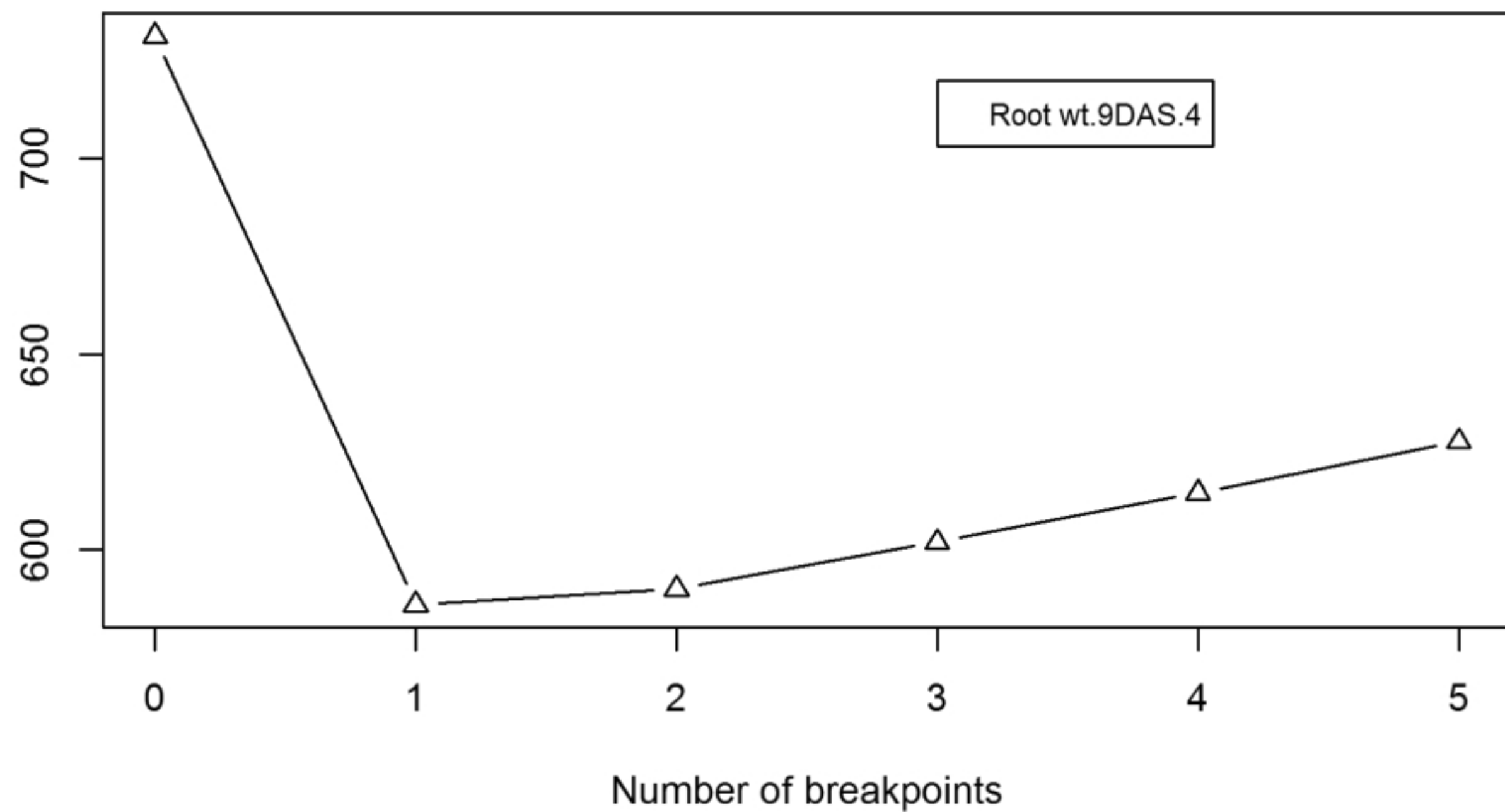
BIC for MSC models with m breakpoints

B

Detected breakpoints for the most parsimonious model

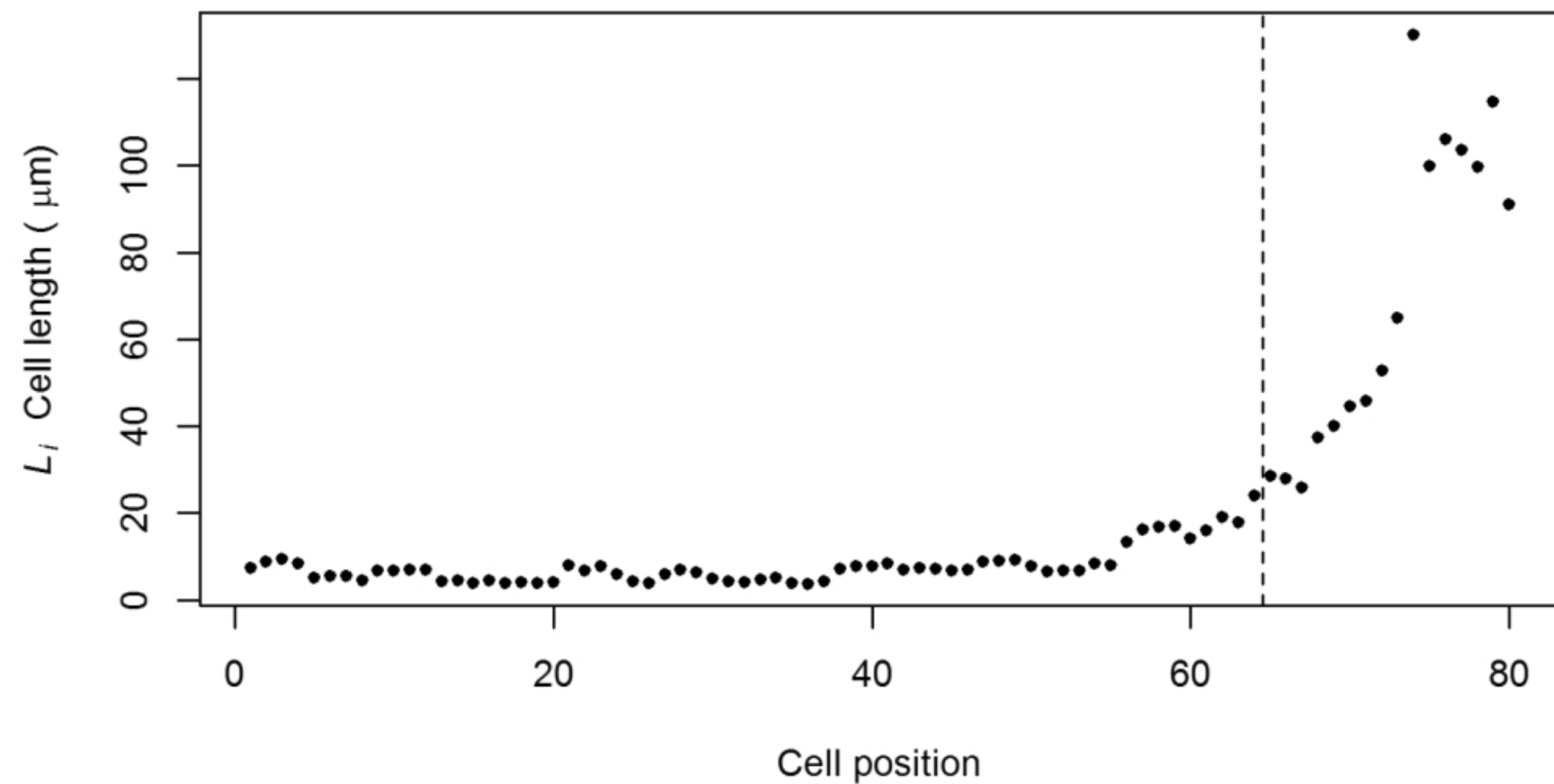


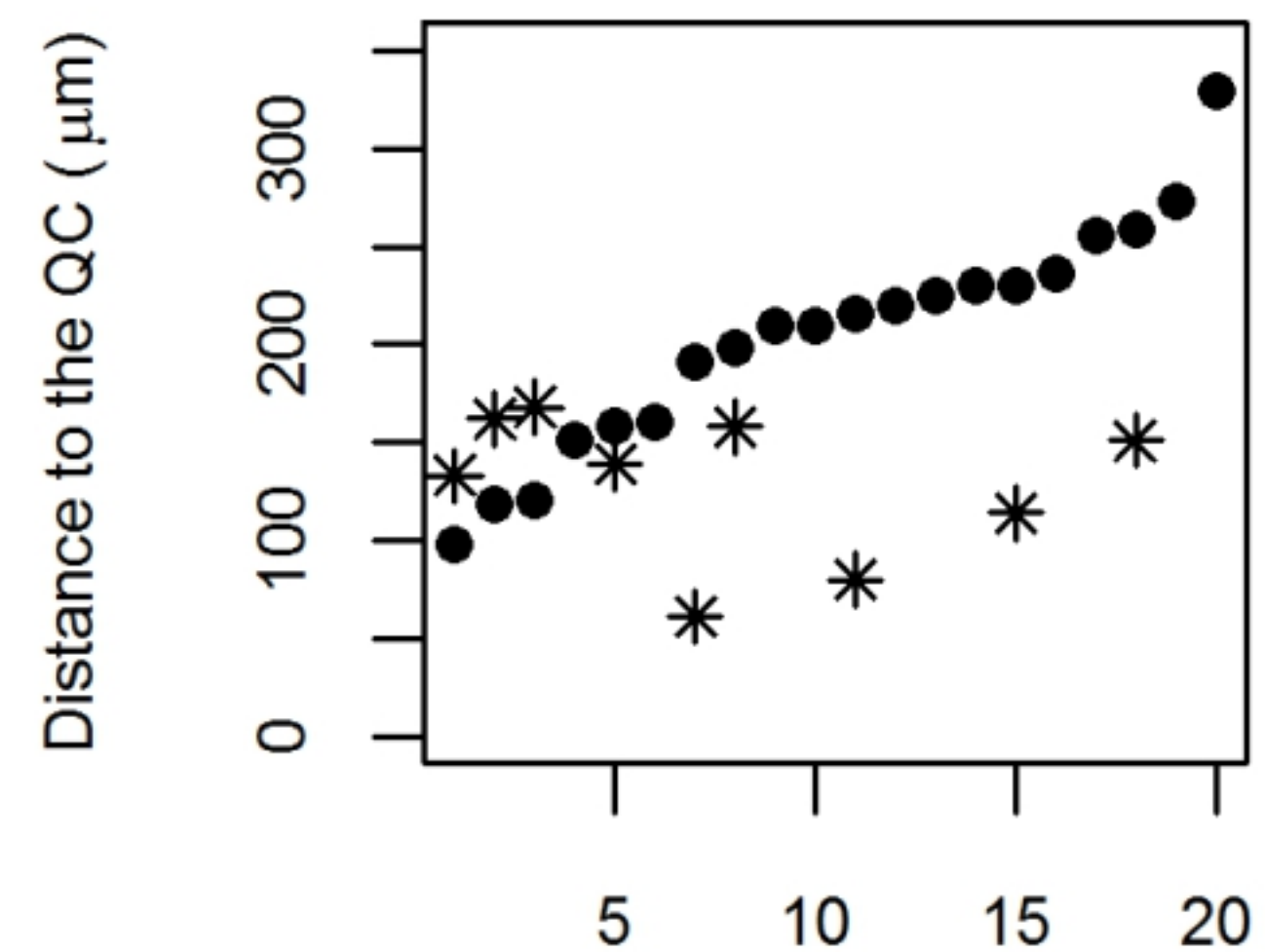
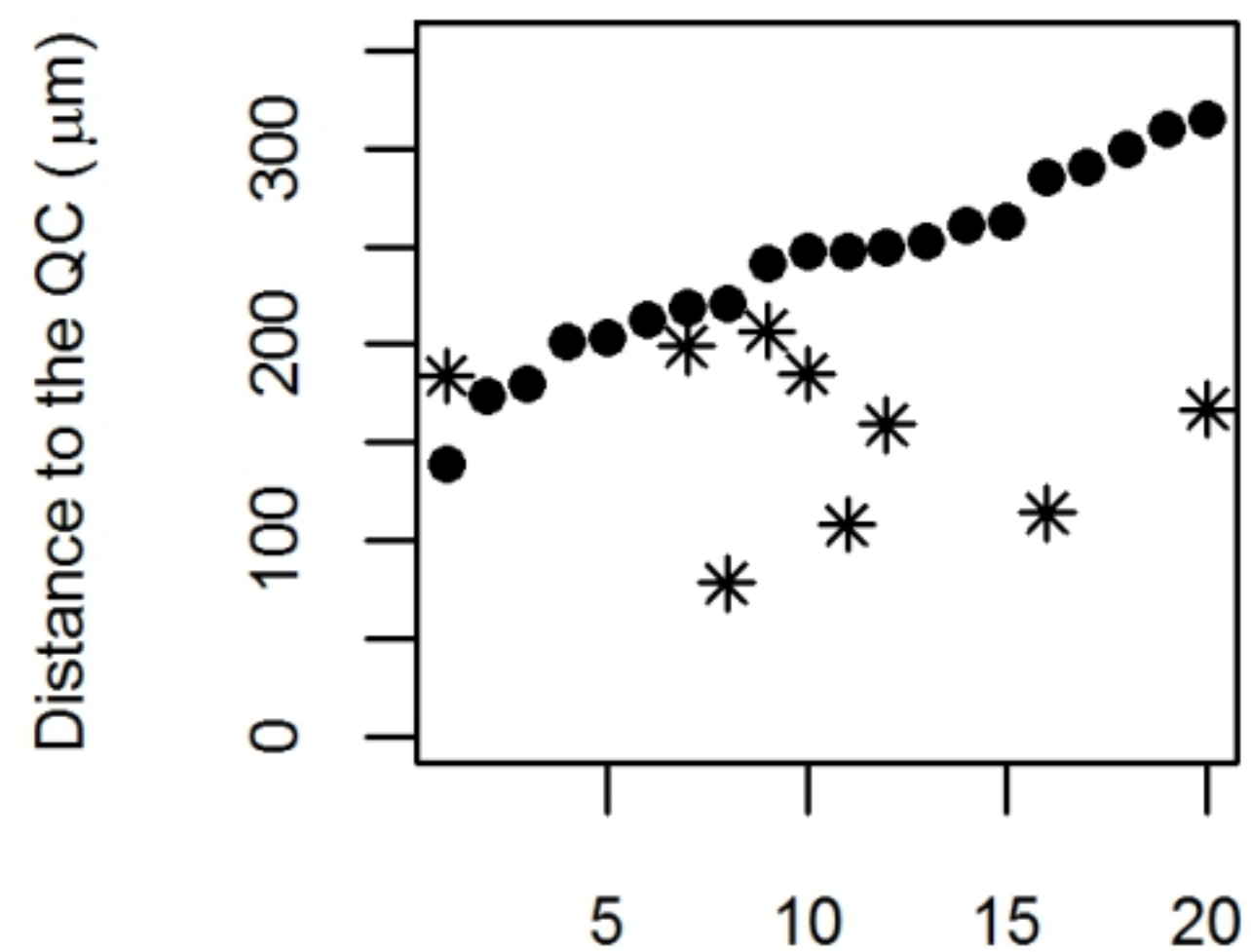
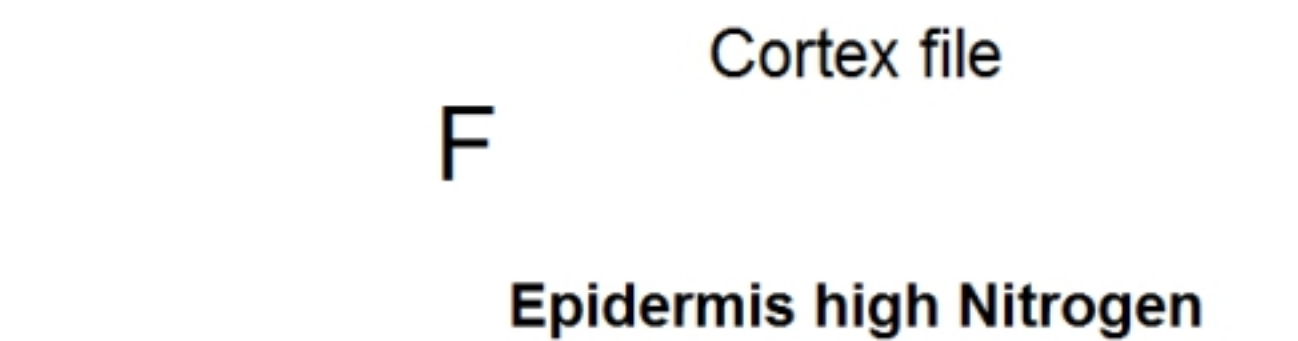
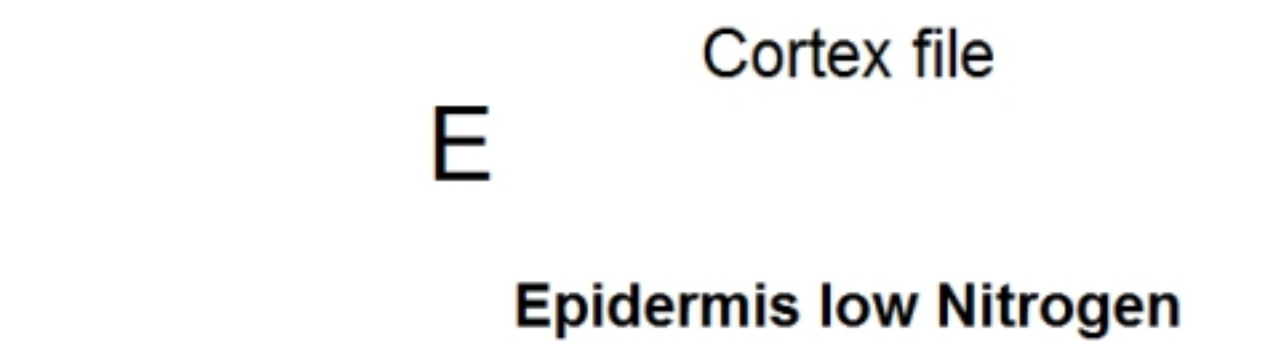
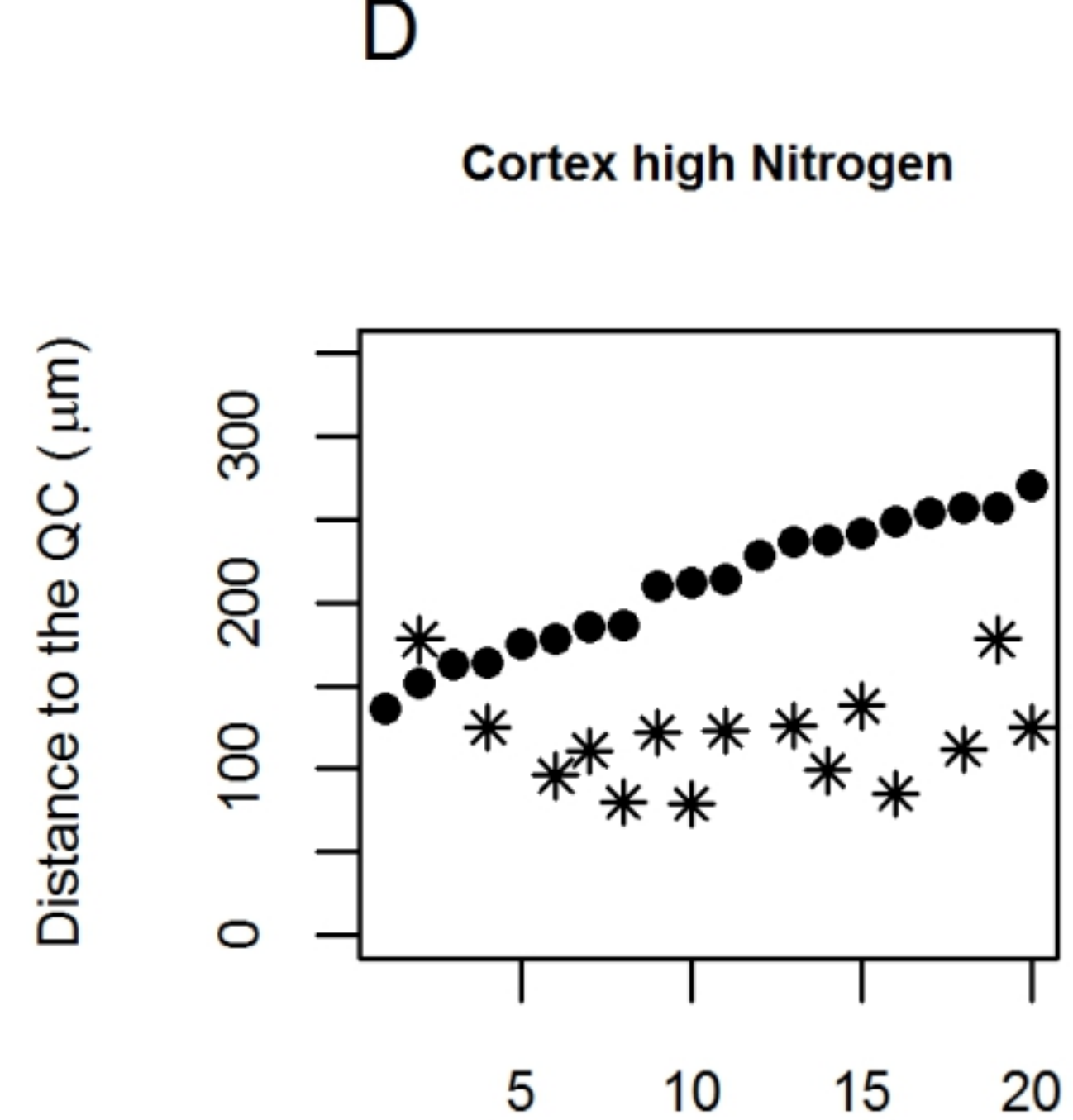
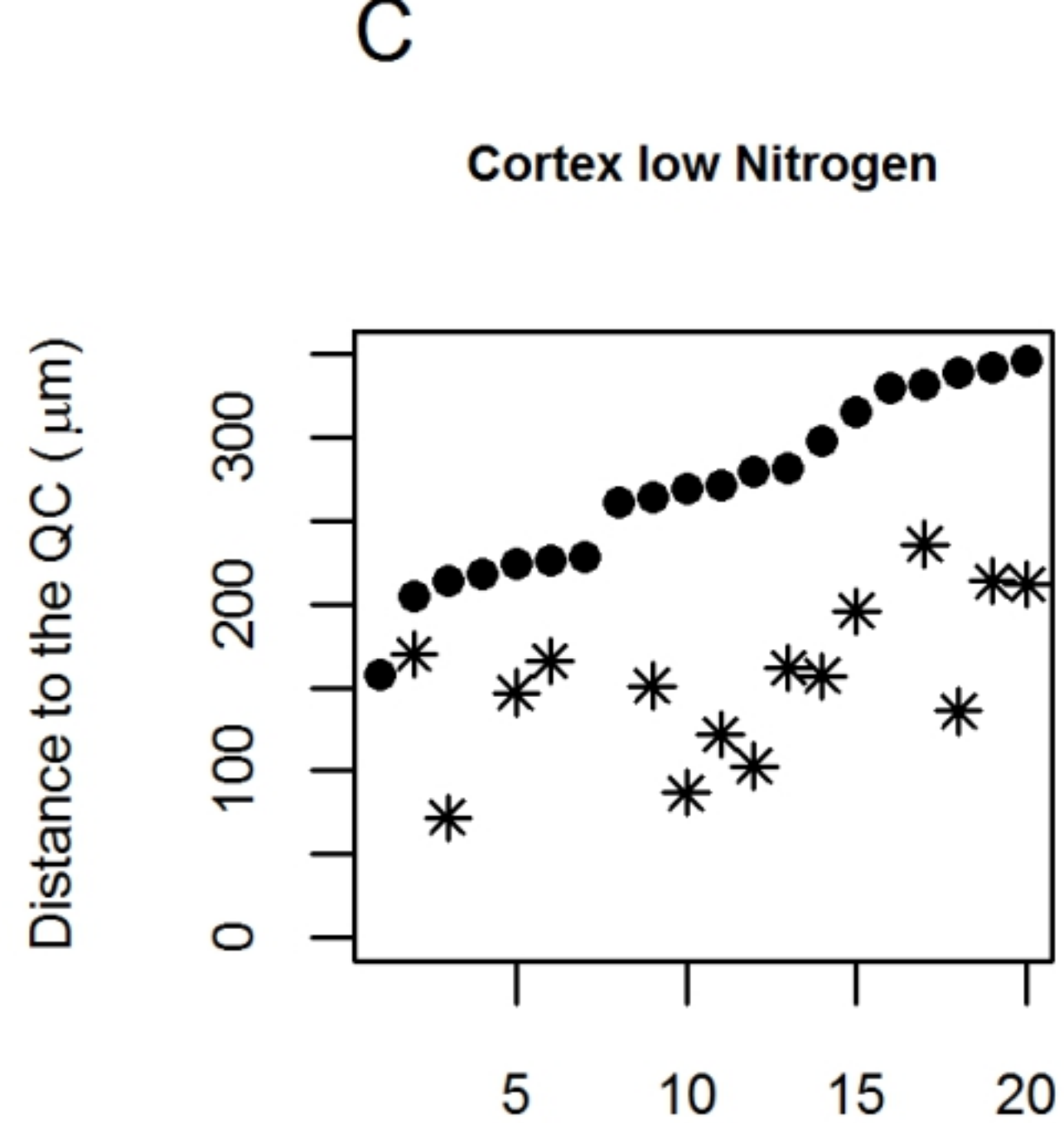
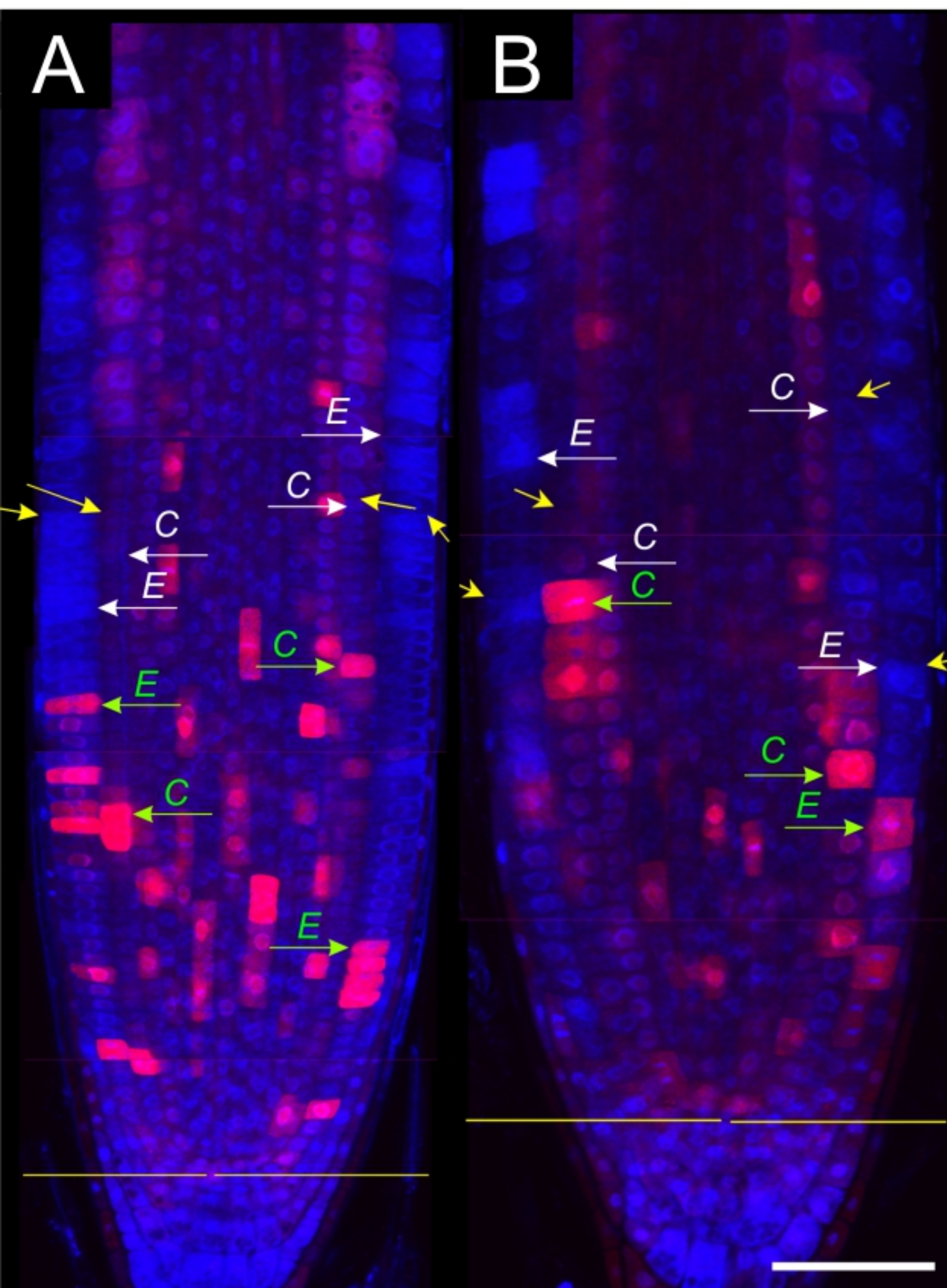
C

BIC for MSC models with m breakpoints

D

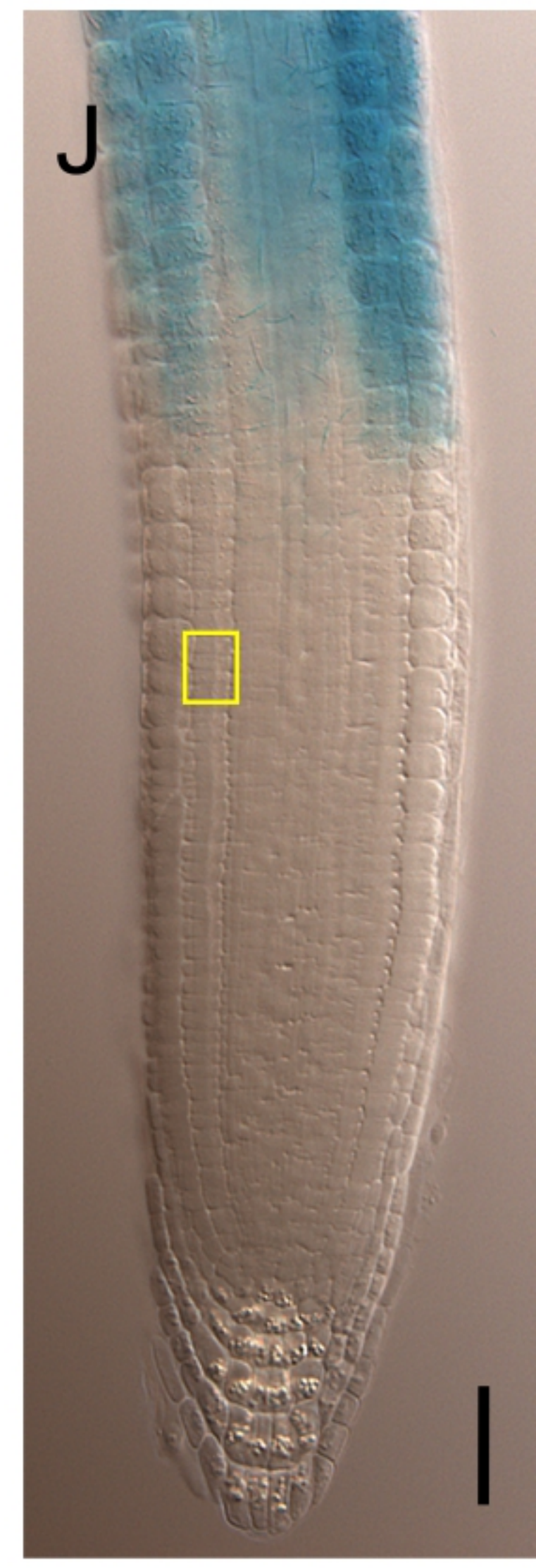
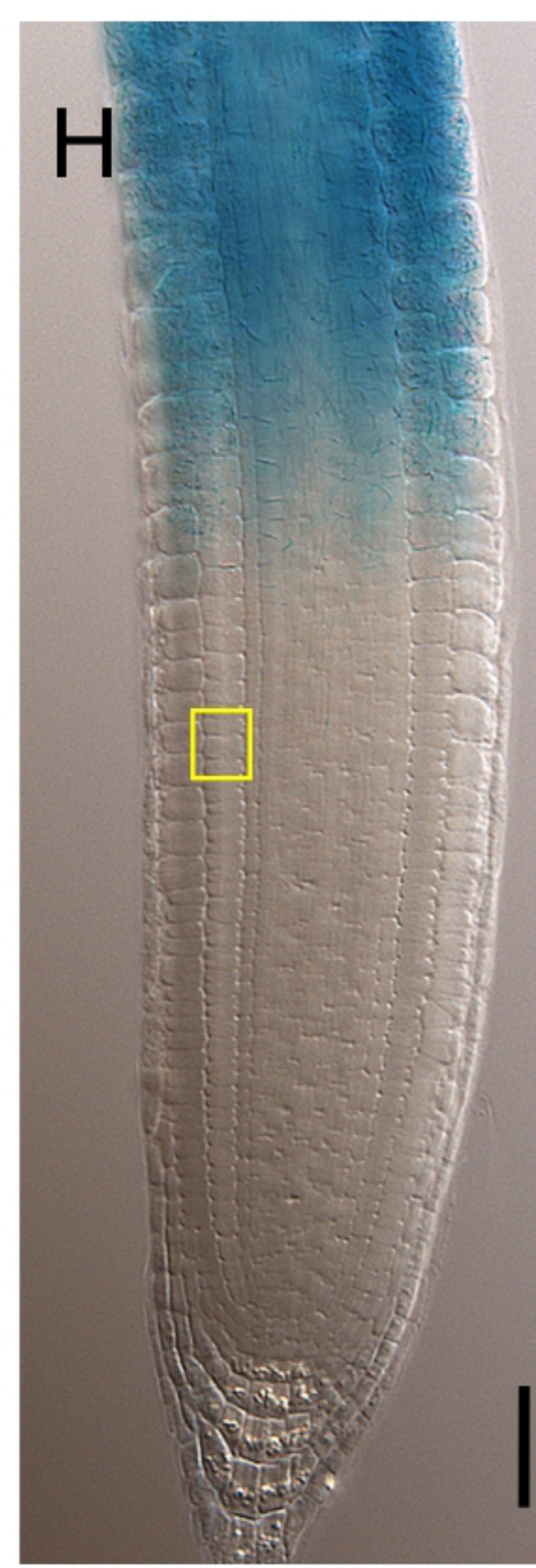
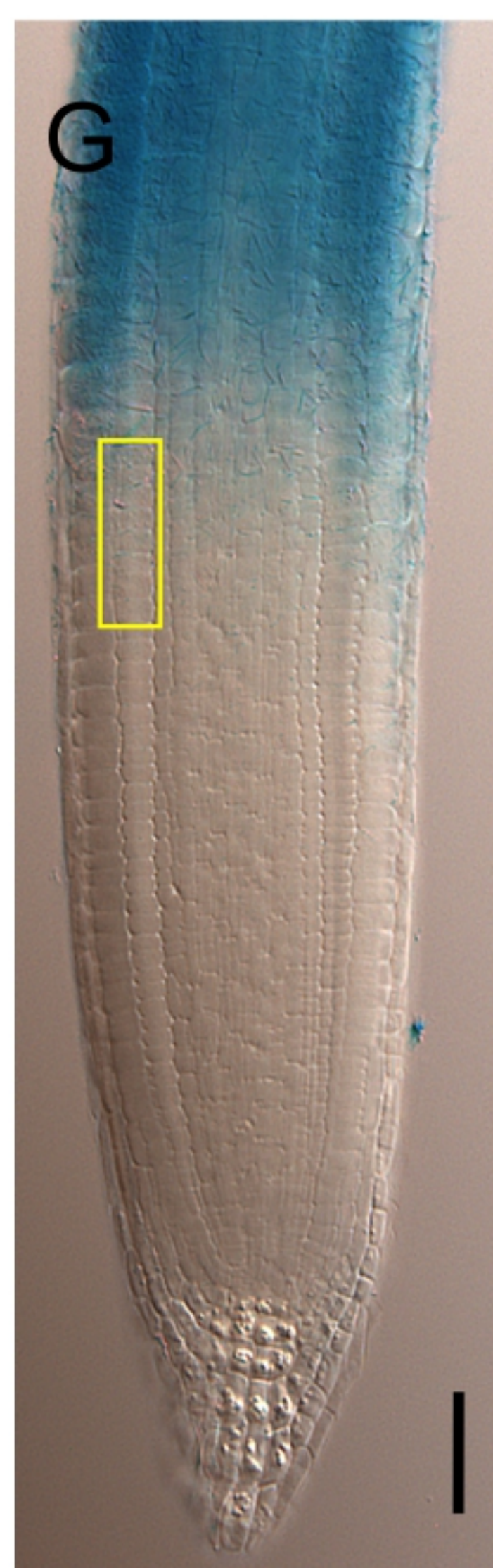
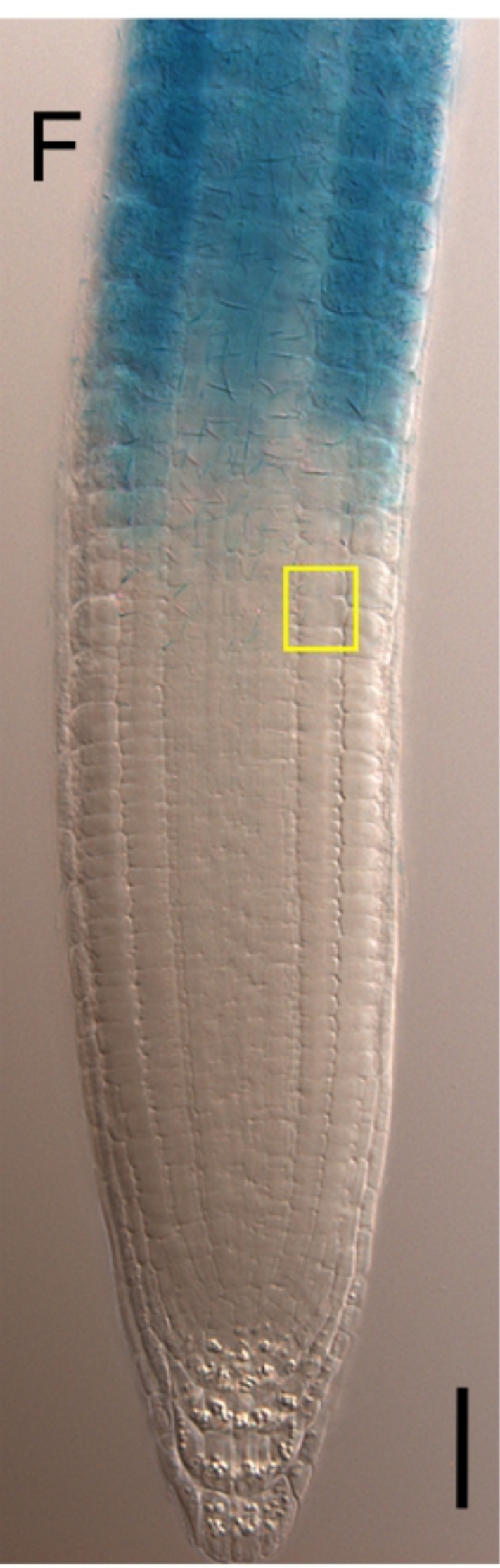
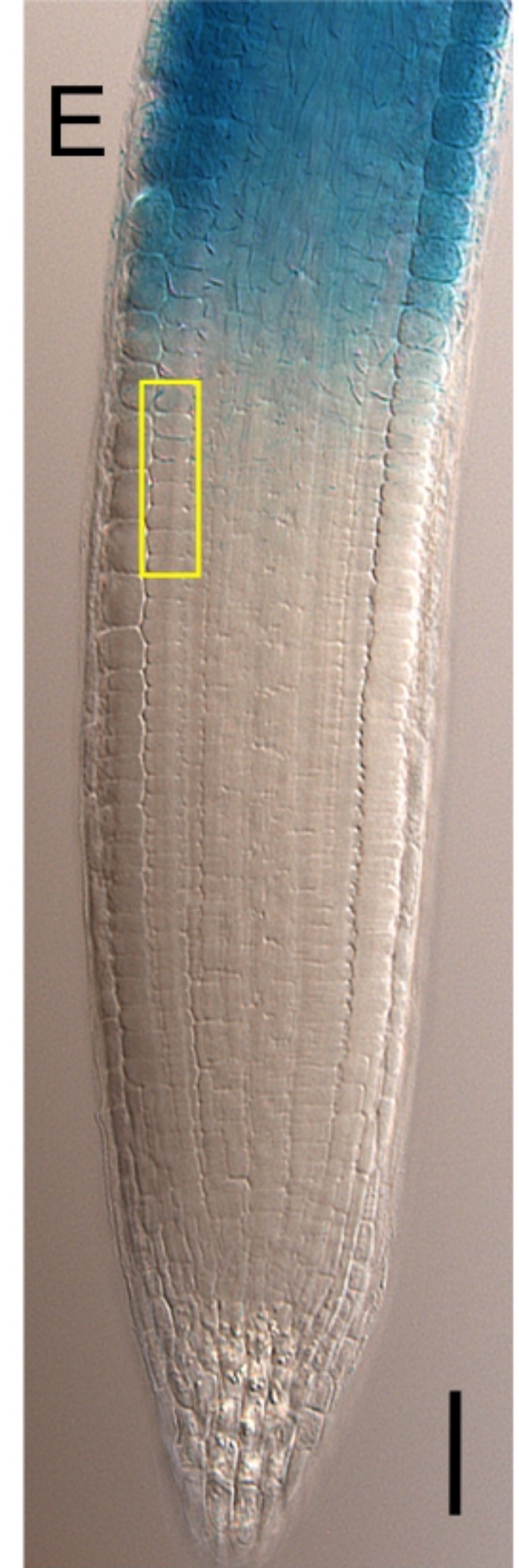
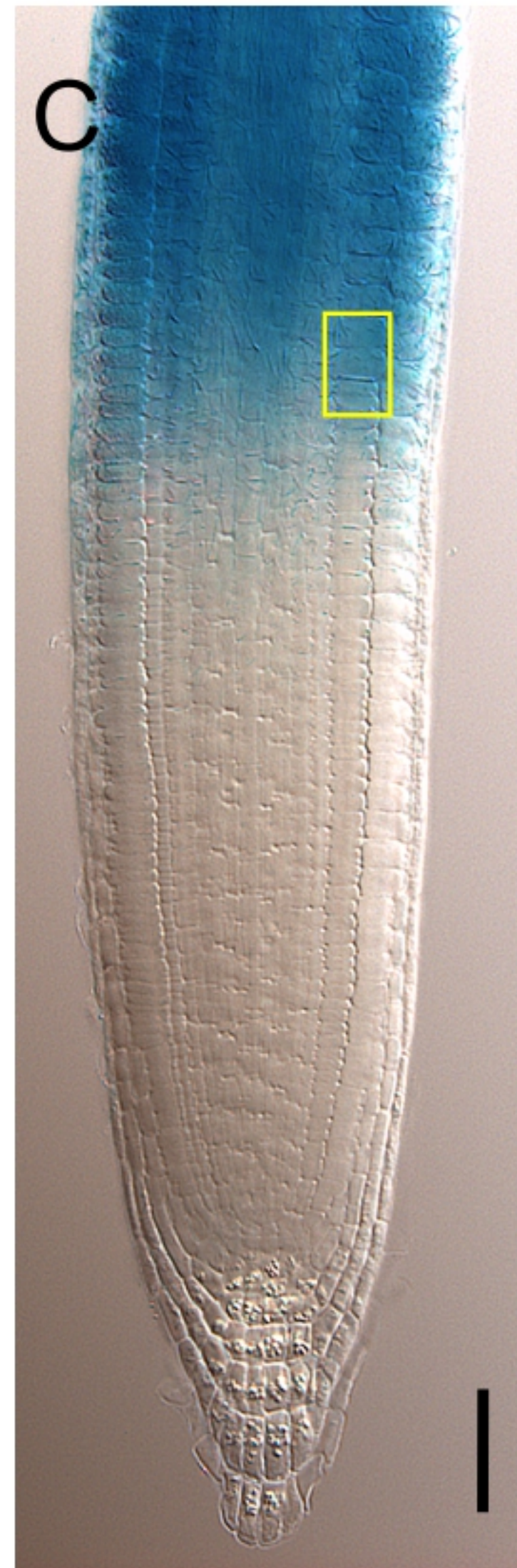
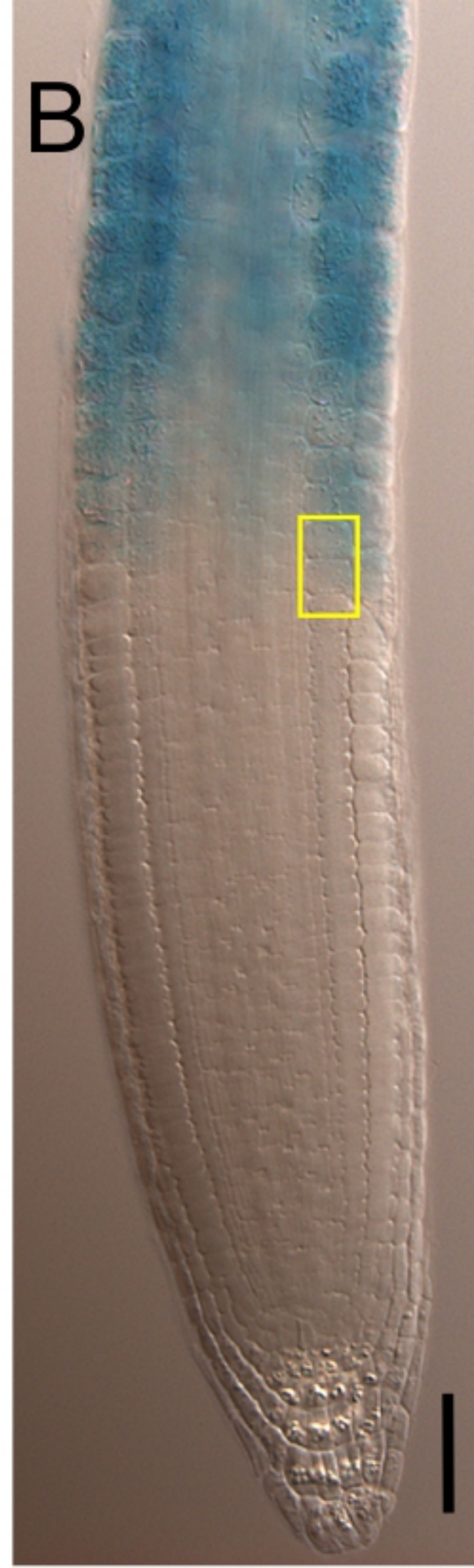
Detected breakpoint for the most parsimonious model

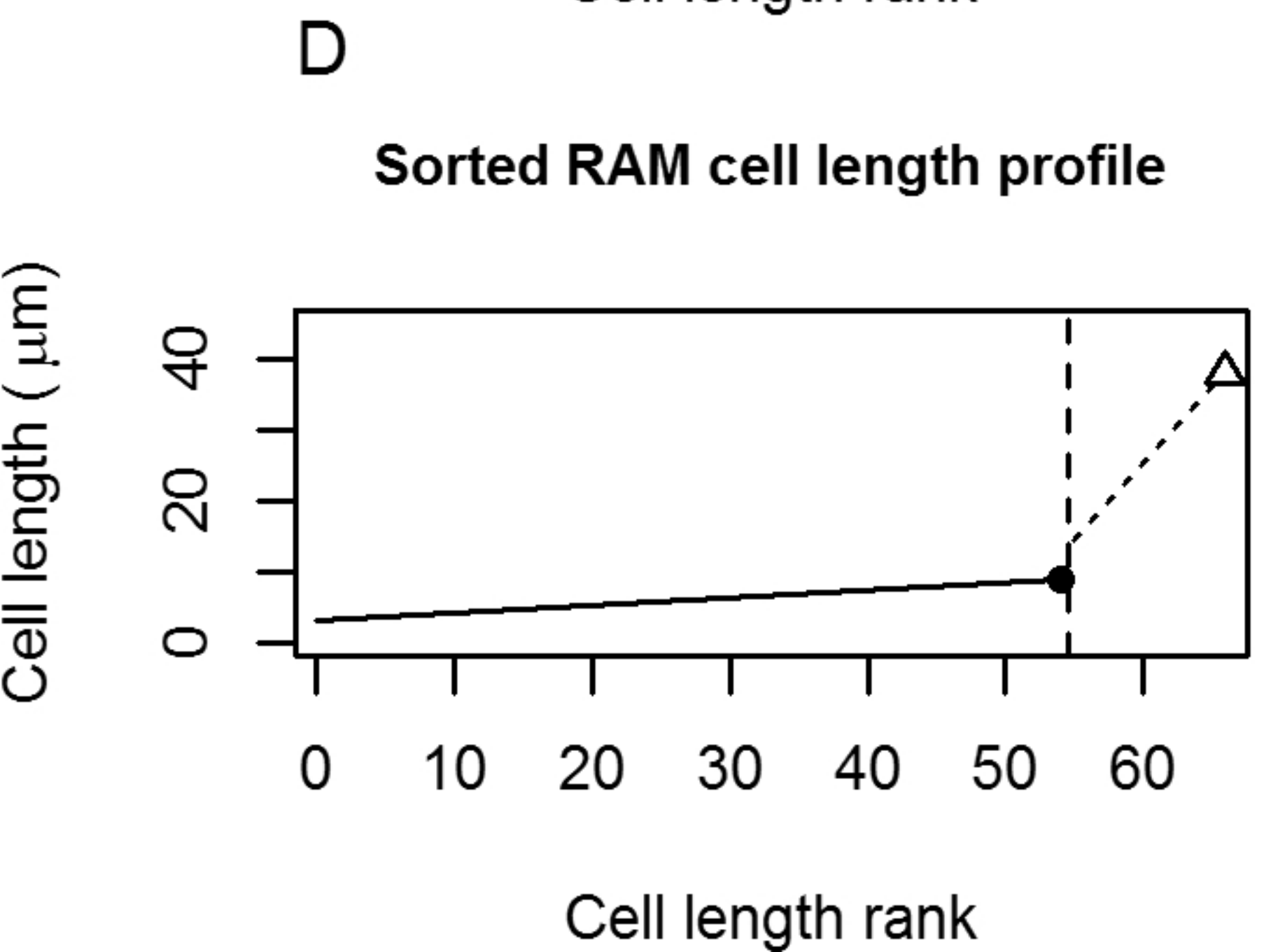
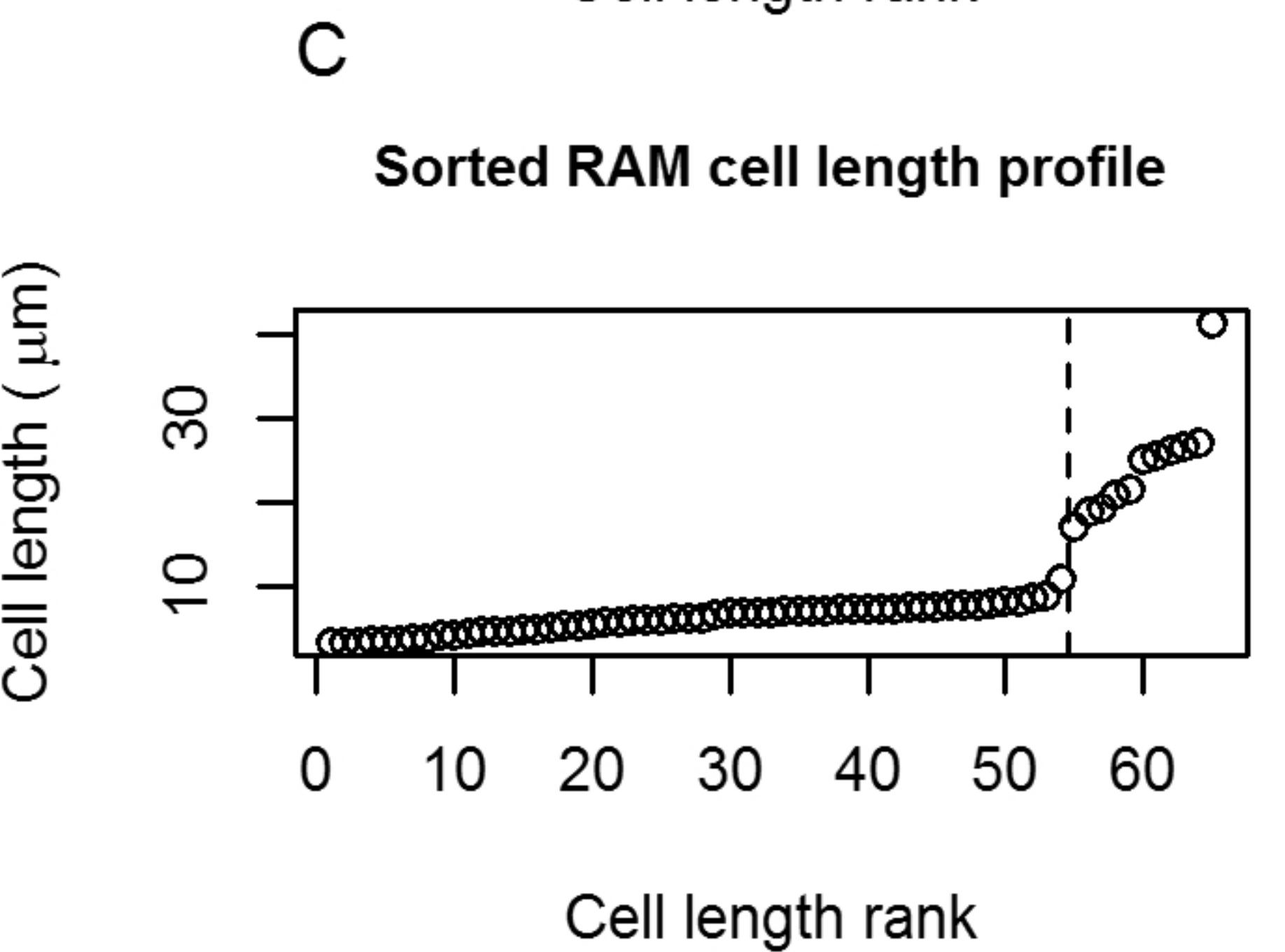
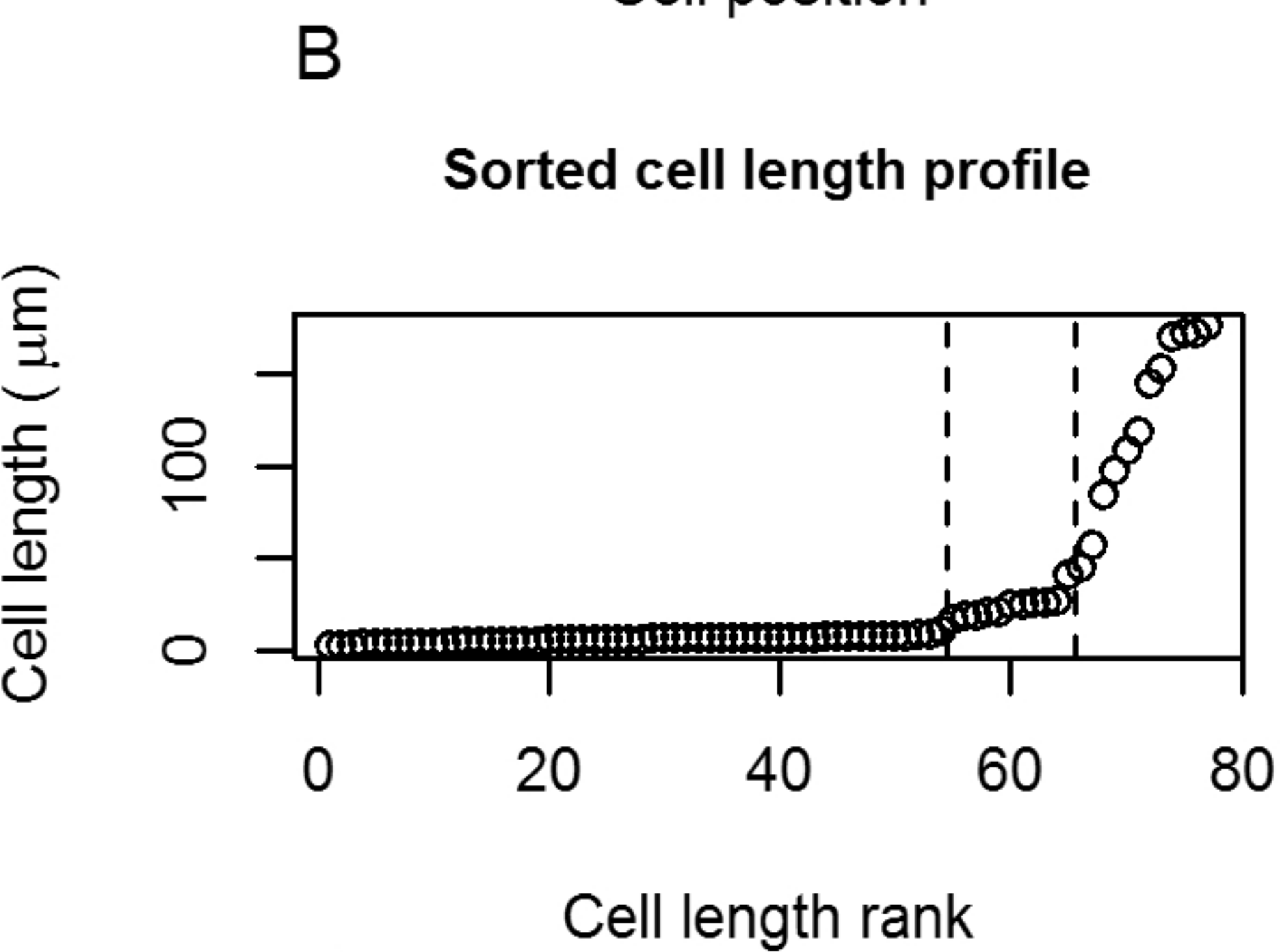
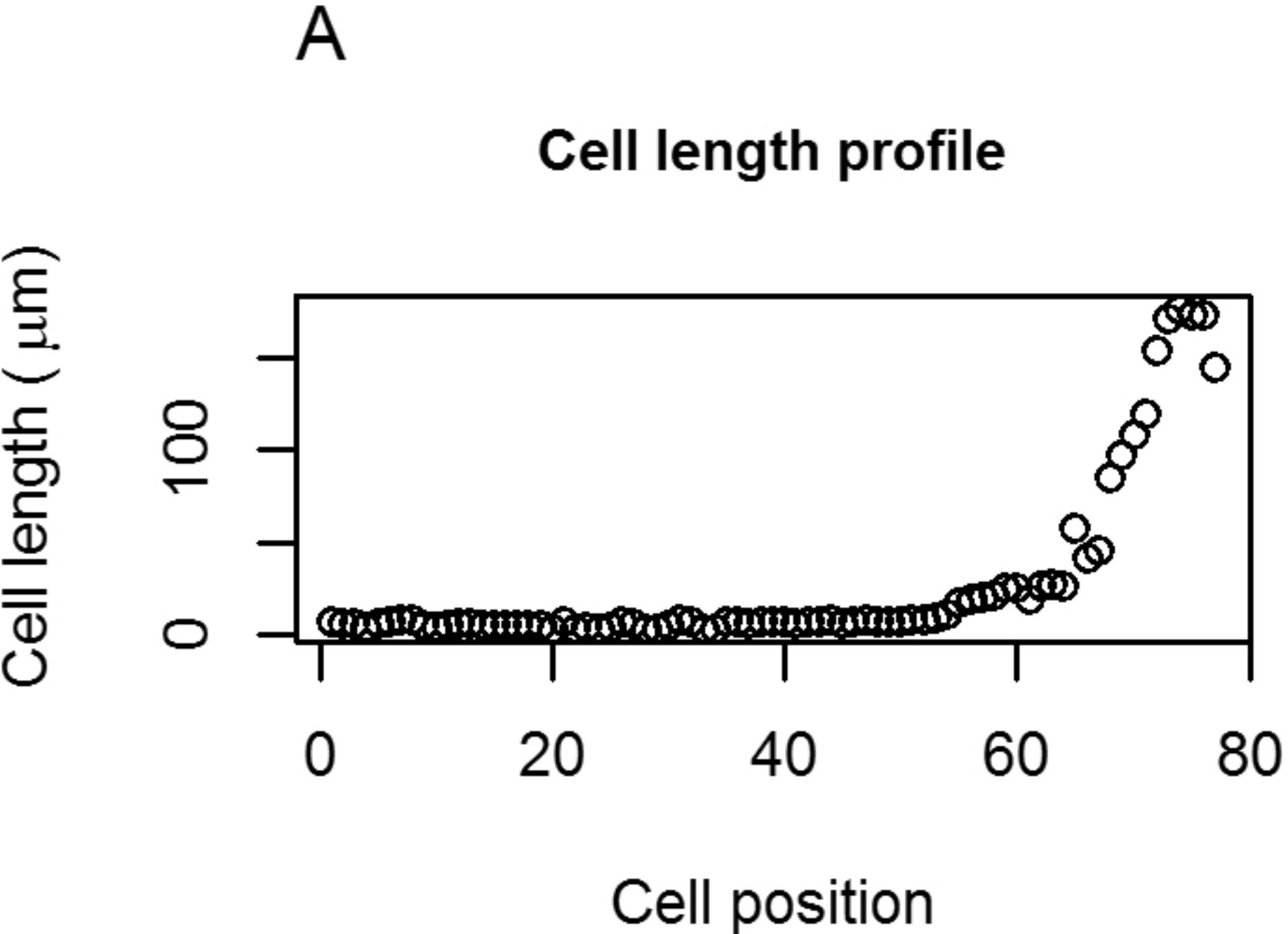




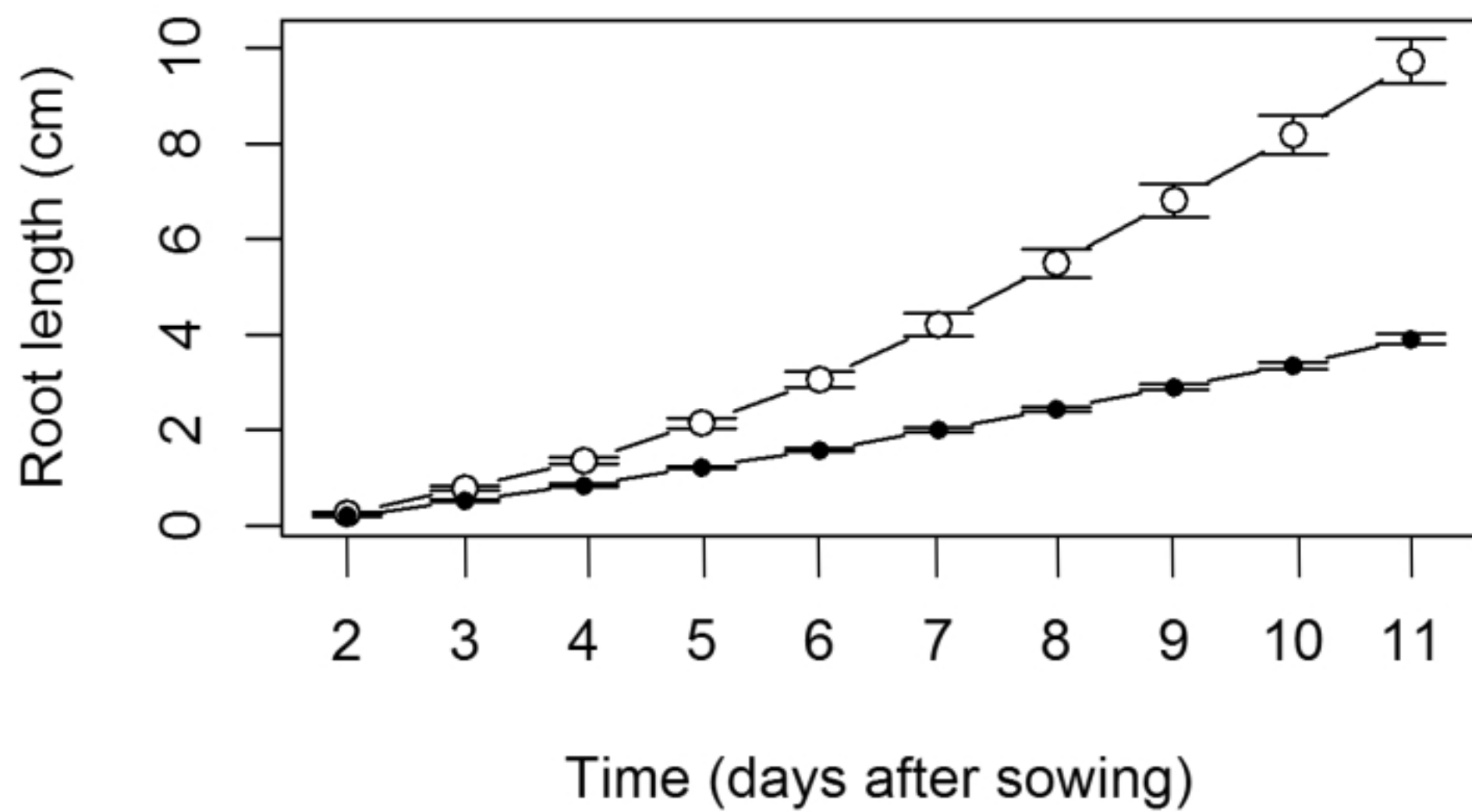
Epidermis file

Epidermis file





A



B

